CHAPTER IV

Optoelectronic Properties of CdSe Thin Films

Chapter IV

Optoelectronic Properties of CdSe Thin Films

4.1 Introduction

The II-VI compounds, both in bulk and thin film forms, shows generally good photosensitivity. For this, these compounds have attracted considerable interests for applications in different optoelectronic devices like light emitting diodes, photo detectors, solar cells etc. Photosensitivity of thin films of the II-VI compounds depends on the over all thin film attributes like the thickness (t) of the films /1/, substrate temperature (T_s) /2/, rate of deposition, source temperature, source to substrate distance etc.

During the growth process itself various native and foreign defects develop in a thin film matrix. Both electrical as well as optical properties of the grown films are influenced to various degrees by these defects. According to Rose /3/ two types of imperfection centers, Class I and Class II can exist in thin films. Class I centers have equal capture cross section for both electrons and holes, and usually take part in the bimolecular recombination processes, whereas the interaction of Class II centers are responsible for the observed linear photoconductivity. Thus so far as the recombination processes are concerned photocurrent versus light intensity curves have a special significance.

The substrate temperature, T_s, is a prominent deciding parameter regarding the grain sizes of the thermally evaporated thin films. In this context it is desirable to study the dark conductivity, photoconductivity, optical absorption, rise and decay of photocurrent etc on the basic of proper characterization of the grain size geometry and distribution pattern built-in in a thin film matrix. Thus a correlative and systematic study on CdSe thin films is essential for creating a comprehensive database in view of the many fold application potentials of this particular class of insulating thin film. Further so far as the optoelectronic properties of the films are concerned most of the already reported works have been done for white light only. Here in this chapter some work on CdSe thin films for threshold wavelength as well as for a range of other monochromatic wavelengths of light covering both sides of the threshold light is reported.

In the photoconductivity of polycrystalline thin films, the localized built-in grain boundary potential barriers play significant roles. The photoconductivity may increase either due to the excess photo generated carriers or increase in carrier mobility or may be due to the both of these processes. Many theoretical models /4-8/ are there to correlate the grain boundary effects in photoconduction processes. Petritz /4/ suggested that photoconductivity results from the change in the majority carrier density in the crystallites and from reduction of grain boundary potential barriers.

Out of the various growth and deposition parameters, T_s is one of the most important factors, depending on which a grown thin film may be either an amorphous or a polycrystalline form. Crystallinity of II-VI thin films improves in general, with the increase of T_s /9/ and it is also possible that a film with optimum electrical properties may be obtained at a certain critical temperature of growth /10/. Thus a detailed study of the physical properties of thin films taking T_s as a variable parameter is necessary to have a proper characterization of a device quality thin film.

Films of polycrystalline nature generally contain grains of various sizes and orientations. As already mentioned such films are usually dominated by different defects like grain boundary dislocations, surface charge layers etc /11/ where conduction is mainly due to ionized impurities, the lattice scattering and the grain boundary scattering /12/. The grain boundaries have a large density of interface states which trap free carriers from the bulk of the grains. Moreover they scatter free carriers by virtue of the inherent disorder and the presence of the trapped charges. The inter face states may be either intrinsic or extrinsic but in both the cases their densities may be changed by exposing the film to appropriate ambients. Interface changes give rise to 'band bending' which is equal to the energy difference between conduction band edges at the grain boundary and in the bulk /13/. Band bending sets up potential barrier between the grains which impedes the flow of current from one crystallite to another. Under illumination due to absorption of light energy in the vicinity of the barrier there occurs neutralization of some of the localized charges responsible for presence of the barrier. As a result the barrier heights are reduced and the current flow between the relatively higher conductivity crystallites increases /14/.

Snejdar and Jerhot /15/ proposed a generalized model for the electrical conductivity in polycrystalline semiconductors assuming that an isotype heterojunction with a certain interface states density existed at the inter grain domain interfaces. According to them carriers may cross the intergrain barriers in three ways viz (a) by tunneling (b) by thermoionic emission and (c) by ohmic conduction. But they still cited Petritz /14/ to justify the act of association of the activation processes with the mobility. According to Petritz primary photoelectric effect is the photon absorption by main band transition and production of electron-hole pairs in the crystallites followed by change in mobility resulting from barrier modulation as a secondary process. Several workers have reported the barrier modulated photoconductivity in CdSe thin films /16-20/.

In the present study CdSe thin films, were grown at T_s in the range 300 to 623K under identical conditions and at elevated T_s polycrystalline growth of films could be achieved. So for the investigation of optoelectronic properties of CdSe thin films at different ambient conditions films grown at elevated T_s are preferred. Similarly keeping the other growth parameters fixed films of thickness mainly in the range 1000 to 3000Å were prepared by keeping different T_s as a growth parameter. In this chapter mostly experimental results of thin films of thickness nearly 2000Å grown at the T_s of 473K are incorporated.

All the grown films were thermally annealed under identical conditions. Thermal annealing was found to improve crystallinity of thin films by changing the grain sizes. Annealing also effects the resistivity of thin films in various ways /21/.

4.2 Experimental Method

4.2.1 Preparation of thin films

For preparing good quality CdSe thin film samples, high quality pure (99.999%) bulk CdSe power obtained from the Koch Light Laboratory, UK, was used. The sample was thermally evaporated at a vacuum of 10^{-6} torr using a tantalum boat, on properly cleaned glass substrates held at different temperatures. The system was then allowed to cool down to the room temperature. In the same vacuum condition the films were then thermally annealed at a definite temperature for a constant interval of time. The CdSe

thin films prepared in this manner were kept in dry desiccators for definite duration of time before being used in experiments.

Before deposition the substrates were properly degassed by keeping these in vacuum inside the coating unit for a certain length of time which is followed by some in-situ preheating. Experimental thin film samples obtained this way are termed as treated films. The films grown on such type of pre heated substrates are found to adhere better to the glass substrate.

The source temperature of the evaporant was kept as low as possible in order to avoid the probable disassociation of the compound /22/. Deposition rate was maintained at 8-12 Å/sec, keeping source to substrate distance 6 cm for uniform deposition of films. Three films were prepared in each pump down cycle for electrical and optical studies. The thickness of the films was measured with the help of a multiple beam interferometer with an accuracy of ±15Å. Aluminium electrodes of proper thickness were vacuum evaporated from a tungsten coil on the treated films leaving a gap of 7mm between the electrodes. Thus an Al/CdSe/Al gap type cell configuration was formed for experimental analysis.

4.2.2 Experimental procedure followed

All optoelectronic measurements were carried out at a vacuum of 10^{-2} torr inside a crowning glass jacket of diameter about 3.5cm. The sample was freely suspended inside the jacket by a specially designed two probe sample holder. The ambient temperature was measured with the help of copper constantan thermocouple and a digital micro voltmeter arrangement. For illumination a 24 volt and 250 watt tungsten halogen lamp with a parabolic reflector was used as a white light source. A series of Carl Zesis (GDR) metal interference filters were used to get monochromatic radiations of wavelength in the range 4000 -10,000Å. The visible region of radiation corresponds to strong optical absorption zone of CdSe thin films. Measurement of light intensity was done with the help of an Aplab sensitive luxmeter (5011 S). Intensity of light used in the experimental work was upto a maximum of 1,50,000 lux. By making the use of two neutral density filters and by using some suitable arrangement in the optical system, the same luxmeter was used for the intensity measurement, even beyond its range of 30,000 lux. In order to avoid the

increase of temperature due to heating by incident radiations, radiations were allowed to fall on the films only for a very short time interval, during which the photocurrent reached its saturation value. An ECIL electrometer amplifier (EA815) with input impedance 10^{14} and higher was used to measure signal currents. Good quality shielded wires were used for electrical connections. The input socket of the electrometer was connected from the sample holder by means of a special antimicrophonic high impedance amphenol cable through a build-in selector switch. The d.c. bias voltage was used within the range (-108V) to (+108V) which was supplied from a series of highly stable 9.0V dry cells. In order to avoid the probable pick-up noise the whole set up along with the observer was housed inside a properly designed and fabricated floating ground Faraday cage. During experimental observations, ambient temperatures were maintained at different values according to the experimental need starting from room temperature to 423K. The complete details of the experimental procedures for the thin film preparation, electrode deposition and measuring technique are elaborated in chapter II.

The structural characterization and film morphology of the films were studied by XRD and SEM analysis, the details of which are presented in chapter III.

4.3 Electrode Contact

Generally aluminium has been used as the electrode material for making ohmic contact with the thermally evaporated CdSe thin films to study the electrical conduction mechanism under different ambient environment by different workers /23-25/. For the same purpose some of the workers have also used other metals. For example Barua et. al. /26,27/ used silver electrodes to get ohmic contact in the low field region with CdSe thin films deposited by thermal evaporation technique.

As already mentioned, in the present experimental work aluminium was use as the electrode material. Before initiating any optoelectronic measurements, the ohmic nature of the electrode contacts was confirmed by recording I-V characteristics at room temperature and also at higher ambient temperatures over a wide range of voltages of both polarities under no illuminations.

Figs 4.1(a to d) show some such plots for films deposited at room temperature and also at different elevated temperatures. Fig 4.1(a) shows the I_D versus V_a

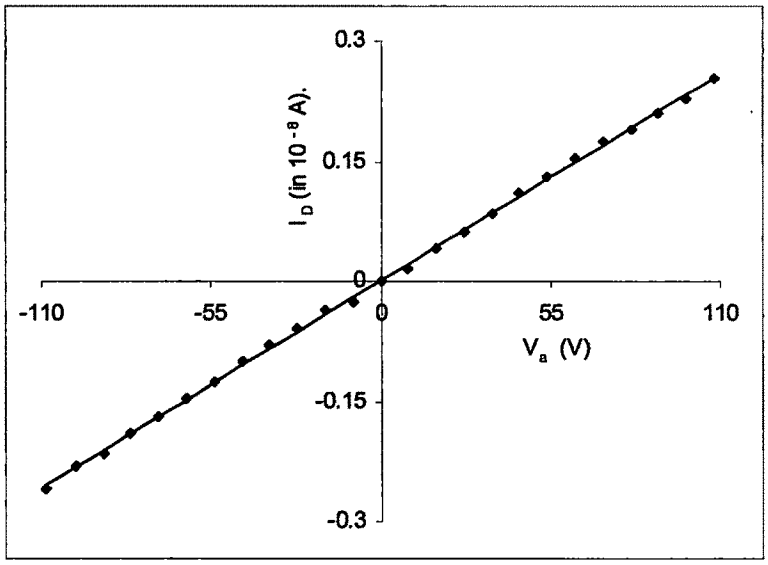

Figure 4.1(a) Dark current (I_D) versus applied bias (V_a) plot of a CdSe thin film of thickness (t = 2150Å) grown at room temperature (T_s = 300K).

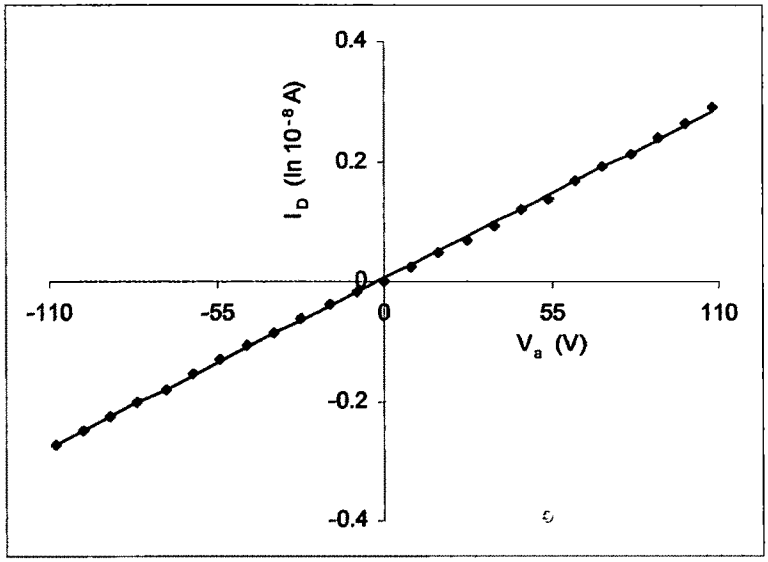

Figure 4.1(b) Dark current (I_D) versus applied bias (V_a) plot of a CdSe thin film of thickness (t = 2000Å) grown at elevated temperature (T_s = 423K).

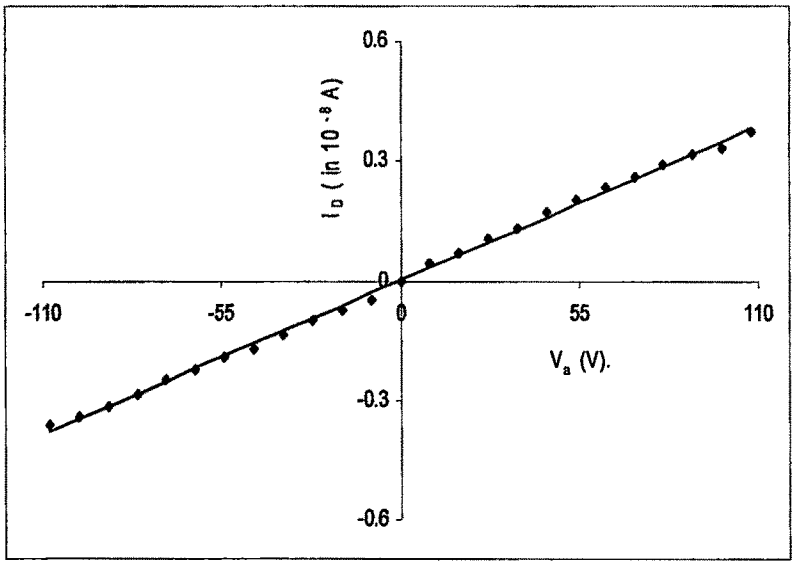

Figure 4.1(c) Dark current (I_D) versus applied bias (V_a) plot of a CdSe thin film of thickness (t = 2000Å) grown at elevated temperature (T_s = 473K).

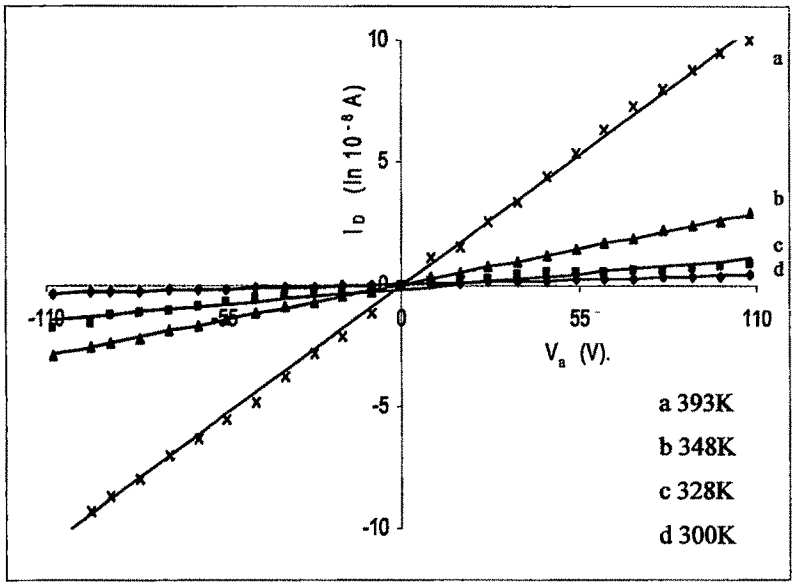

Figure 4.1(d) Dark current (I_D) versus applied bias (V_a) plots at different ambient temperatures of a CdSe thin film (t = 1750Å) grown at T_s = 473K.

characteristics plot for a film deposited at room temperature, where I_D is the dark current and V_a is the applied bias voltage. The plot is symmetrical and linear about the zero of applied voltage for the entire range of applied bias (-108V) to (+108V). This means that the electrode contacts are ohmic and there develops no rectifying barrier at the electrode thin film junction in the complete range of applied voltages for dark conductivity.

From the plot of Fig 4.1(d), which is for a film deposited at an elevated T_s of 473K, it is observed that under different ambient conditions of temperature also the variation of dark current against applied bias is linear within the range of applied bias (-108V) to (+108V). Similarly for films grown at other elevated temperatures and having different thickness also the linear nature of dark current persists for both +ve and –ve bias conditions, as shown in Fig 4.1(b) and Fig 4.1(c) for films deposited at T_s = 373K & 473K respectively and studied at room temperature environment.

4.4 Characteristic plots of photocurrent

The variation of photocurrent against different applied bias in CdSe thin films was observed under different ambient conditions of intensity as well as wavelength of light. Such plots are shown in the Fig 4.2(a) and Fig 4.2(b) for a typical film of thickness 2000Å grown at T_s = 473K.

The plots of Fig 4.2(a) show the variation of photo current I_{ph} with applied bias V_a under monochromatic illuminations of constant intensity for five different wavelengths of light; where by definition photocurrent $I_{ph} = I_L - I_D$, I_L is the current under illumination and I_D is the dark current. Fig 4.2(b) shows a similar type of plot under five different intensities for the monochromatic illumination of 725nm. I_{ph} versus V_a characteristics for films of same thickness but grown at different T_s and also for films of different thickness but grown at constant T_s under monochromatic illumination of 725 nm of constant intensity are shown in Figs 4.2(c, d) and Figs 4.2(e, f) respectively.

From the plots it is clearly observed that I_{ph} versus V_a characteristics obey two distinct conductivity regions. There is a range of low voltage (for both polarities) where the variations of I_{ph} versus V_a are linear and pass symmetrically through the origin. Hence in the low field region the conduction mechanism is ohmic. But beyond this particular range of voltage it is found that I_{ph} increases with the applied bias V_a nonlinearly. Such

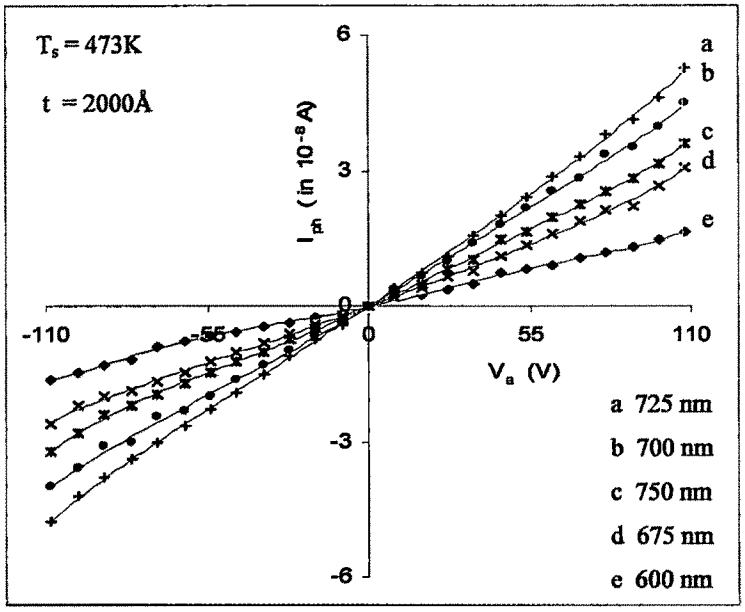

Figure 4.2(a) Photocurrent (I_{ph}) versus applied bias (V_a) plots of a CdSe thin film grown at elevated T_s illuminated by different monochromatic lights.

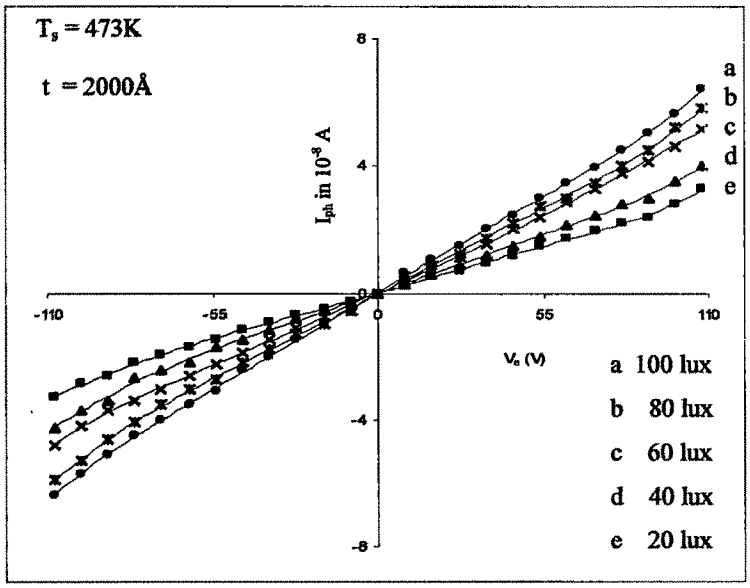

Figure 4.2(b) Photocurrent (I_{ph}) versus applied bias (V_a) plots of a CdSe thin film grown at elevated T_s illuminated by monochromatic light of 725 nm.

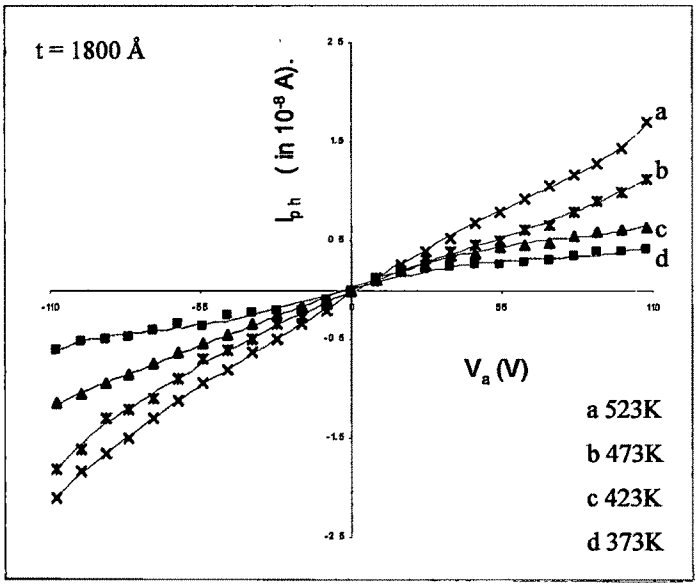

Figure 4.2(c) Photocurrent (I_{ph}) versus applied bias (V_a) plots of CdSe thin films grown at different T_s and illuminated by monochromatic light of 725nm.

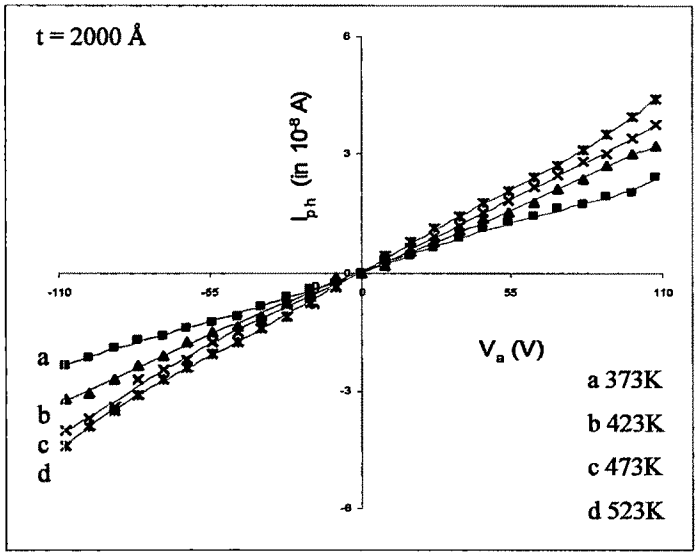

Figure 4.2(d) Photocurrent (I_{ph}) versus applied bias (V_a) plots of CdSe thin films grown at different T_s and illuminated by monochromatic light of 725nm.

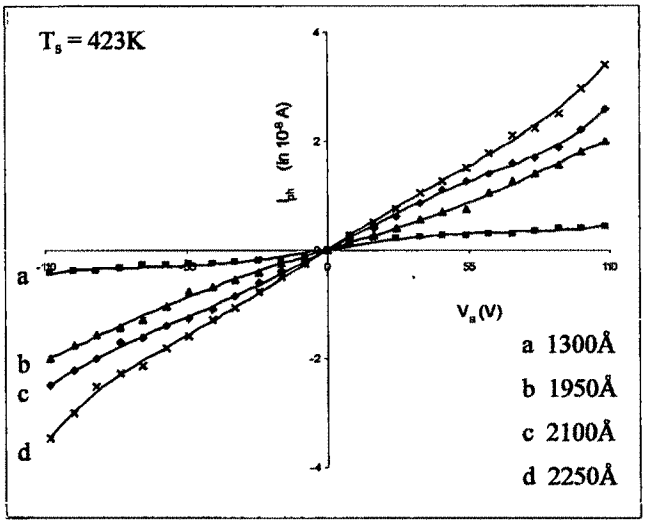

Figure 4.2(e) Photocurrent (I_{ph}) versus applied bias (V_a) plots of CdSe thin films of different, t, and illuminated by monochromatic light of 725nm.

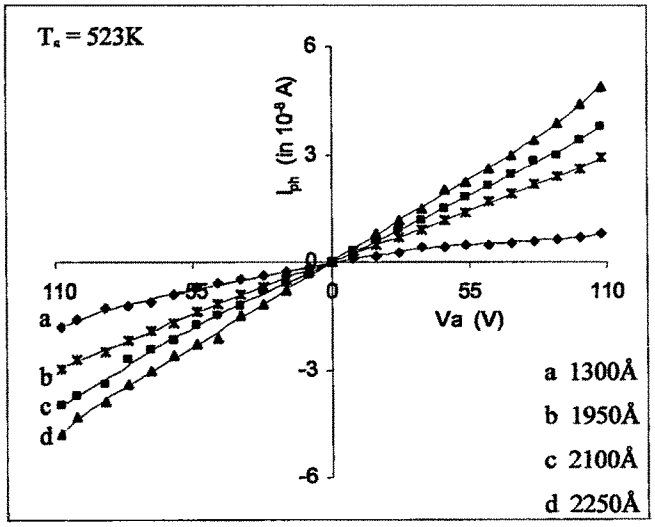

Figure 4.2(f) Photocurrent (I_{ph}) versus applied bias (V_a) plots of CdSe thin films of different, t, and illuminated by monochromatic light of 725nm.

non linear dependence of I_{ph} with applied bias points towards Poole- Frenkel or Schottky effects /26, 28, 29/. Now since in the present case the electrode semiconductor contacts were ohmic, the results can be interpreted in terms of Poole- Frenkel effect.

4.4.1 The effect of field

Poole Frenkel effect

The Poole-Frenkel effect is the lowering of built-in potential barriers inside a sample while interacting with an applied electric field /30/. At a metal insulator interface the potential step changes smoothly as a result of image force. The force arises because the metal surface becomes polarized (positively charged) by escaping electrons, which in turn exerts an attractive force $e^2/16\pi\varepsilon_o\varepsilon^* x^2$ on the electron. So the potential energy of the electron due to image force is

$$\Phi_{im} = - e^2/16\pi\varepsilon_o\varepsilon^* x \qquad (4.1)$$

where x is the distance of the electron from the electrode surface, ε^* is the frequency dependent dielectric constant. Image force effects play an important role in the conduction process when the current is electrode limited. The potential energy of an electron in a Coulombic field is given by

$$\Phi_{cf} = -e^2/4\pi\varepsilon_o\varepsilon^* x \qquad (4.2)$$

which is four times that due to image force effects. When an electric field exists at a metal insulator interface, it interacts with the image force and lowers the potential barrier. The change $\Delta\Phi_s$ in the barrier height due to interaction of the applied field with the image potential is given by

$$\Delta\Phi_s = (e^3/4\pi\varepsilon_o\varepsilon^*)^{1/2}F^{1/2} = \beta_s F^{1/2} \qquad (4.3)$$

The Poole-Frenkel attenuation of a Coulombic barrier, $\Delta\Phi_{PF}$, in a uniform electric field is twice that due to the Schottky effect at a neutral barrier

$$\Delta\Phi_{PF} = (e^3/\pi\varepsilon_o\varepsilon^*)^{1/2}F^{1/2} = \beta_{PF}F^{1/2} \qquad (4.4)$$

In short, $\Delta\Phi_{PF} = 2\Delta\Phi_S$

This result was first applied by Frenkel to the host atoms in bulk semiconductors and insulators /30/.

The observed conductivity in thin film insulators is due to extrinsically rather than intrinsically bulk generated carriers. The intrinsic current density in a semiconductor is given by

$$I = e\mu N_c F \exp(-E_g/2kT) \tag{4.5}$$

where e is the electronic charge, μ is the mobility, F is the field in the semiconducting material, N_c effective density of states in the insulator, E_g is the energy gap, k is Boltzmann's constant, T is the ambient temperature in degree Kelvin.

Frenkel argued that in the presence of uniform field the band gap energy E_g in a solid is lowered by an amount given by equation (4.4). Thus conductivity is obtained by substituting $(E_g - \Delta\Phi_{PF})$ for E_g in equation (4.5). Hence

$$I/F = e\mu N_c \exp\{-(E_g - \Delta\Phi_{PF})/2kT\}$$

$$I/F = e\mu N_c \exp(-E_g/2kT)\exp(\beta_{PF}F^{1/2}/2kT)$$

So the field dependent conductivity is of the form

$$\sigma = \sigma_o \exp(\beta_{PF}F^{1/2}/2kT) \tag{4.6}$$

where $$\sigma_o = e\mu N_c \exp(-E_g/2kT)$$

Equation (4.6) may be written in the form

$$J = J_o \exp(\beta_{PF}F^{1/2}/2kT) \tag{4.7}$$

Here σ_o is the low field conductivity and $J_o = \sigma_o F$ is the low field current density. Because of image force lowering of the barrier, the electrode-limited current doesn't saturate according to the Richardson law,

$$J = AT^2 \exp(-\Phi_o/kT) \tag{4.8}$$

where $A = 4\pi em(kT)^2/h^2$

It rather obeys the Richardson Schottky law

$$J = AT^2\exp\{-(\Phi_o-\Delta\Phi_s)/kT\} = AT^2\exp(-\Phi_o/kT)\exp(\beta_s F^{1/2}/kT) \quad (4.9)$$

Although $\Delta\Phi_{PF} = 2\Delta\Phi_s$, the coefficient of $F^{1/2}$ in the exponential is the same as for both Richardson-Schottky (at neutral contact) and Poole-Frenkel current density versus electric field characteristics, i.e.

$$\beta_{PF} = 2\beta_s \quad (4.10)$$

Mead suggested /30/ that since the traps abound in an insulator and that a trap having a Coulombic type barrier would experience the Poole-Frenkel effect at high fields, there by increasing the probability of escape of an electron immobilized therein, the current density in thin film insulators containing shallow traps is given by

$$J = J_o\exp(\beta_{PF}F^{1/2}/kT) \quad (4.11)$$

In this case the coefficient of $F^{1/2}$ is twice that in equation (4.7). Mead first reported the field dependent conductivity apparently in the form given by (4.11). (4.11) is the usual form of Poole-Frenkel equation associated with thin film insulators, rather than that given by (4.7).

Due to illumination, grain boundary potential barrier Φ_b is reduced which results in enhancing the effective mobility given by

$$\mu^* = \mu_o\exp(-e\Phi_b/kT_o) \quad (4.12)$$

where T_o is the characteristics temperature of the film system, μ_o is the mobility of the carrier with no barrier effect /4/.

As the intensity of illumination, Φ increases, increasing number of photo generated carriers become effective in reducing the grain boundary barrier height Φ_b This effect is called barrier modulation. As a result effective mobility increases exponentially with illumination. In this case

$$\mu^* = f(\Phi)$$

since $$\Phi_b = f(\Phi)$$

Thus the effective mobility contributes another exponential factor to the Poole-Frenkel conductivity. So the effective Poole-Frenkel conductivity increases with illumination. The effective current density may be written as

$$J_{ph} = n\, e\, F\, \mu_o \exp\{(\beta_{PF} F^{1/2} T_o - e\, \Phi_b\, T) / k\, T\, T_o)\} \qquad (4.13)$$

where n is the majority photogenerated carrier density. So for other ambient parameters remaining fixed, the photocurrent density increases exponentially with illumination Φ. Expression (4.13) is the resultant due to both Poole-Frenkel effect and the barrier modulation effect due to illumination. In fact the barrier modulation process is the resultant of two contributions one from applied bias and other from illumination.

The plot of ln J_{ph} versus $F^{1/2}$ of different CdSe thin films are shown in Figs 4.3(a to f), the graphs are found to be linear in high field regions which indicate the predominance of Poole-Frenkel type of conduction mechanism at high fields. From the slope m = β_{PF} / kT of the plots, the values of Poole-Frenkel coefficient were calculated. The β_{PF} values calculated from this relation for CdSe thin films deposited at elevated T_s and studied under different ambient conditions are presented in Table 4.1(a) and Table 4.1(b).

Table 4.1(a) Calculated values of Poole-Frenkel coefficients (β_{PF}) in 10^4 eV $V^{-1/2} m^{1/2}$ unit for a CdSe film of t = 2000Å and grown at T_s = 473K, illuminated by different monochromatic lights.

Intensity of illumination	Wavelength of monochromatic illumination				
	600nm	675nm	750nm	700nm	725nm
50 lux	5.770	5.459	5.407	5.278	5.226
Wavelength of illumination	Intensity of monochromatic illumination				
	20 lux	40 lux	60 lux	80 lux	100 lux
725nm	5.899	5.614	5.563	5.563	5.226

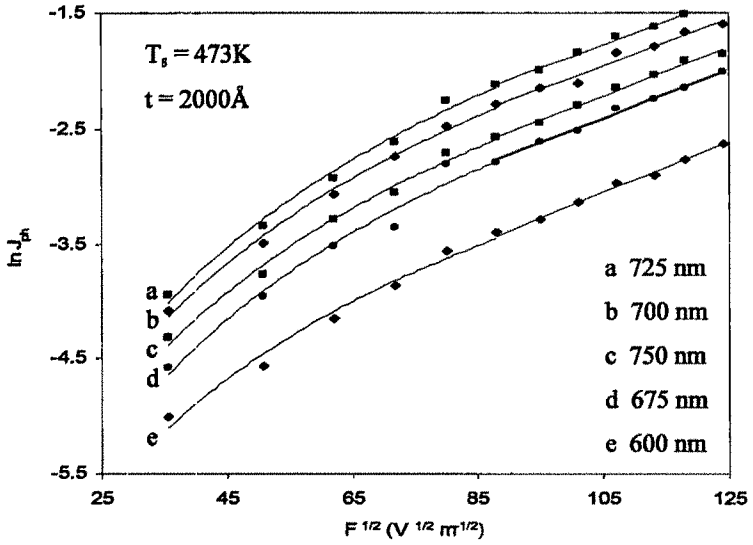

Figure 4.3(a) $\ln J_{ph}$ versus $F^{1/2}$ plots of a CdSe thin film illuminated by different monochromatic lights of constant intensity.

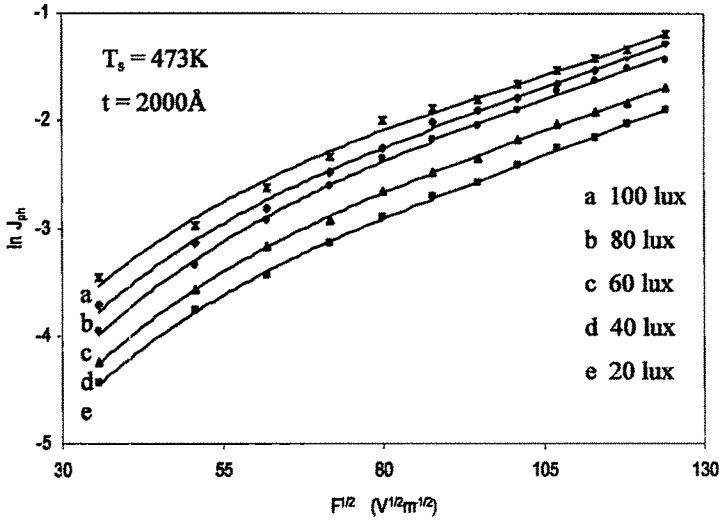

Figure 4.3(b) $\ln J_{ph}$ versus $F^{1/2}$ plots of a CdSe thin film illuminated by monochromatic light (725nm) of different intensities.

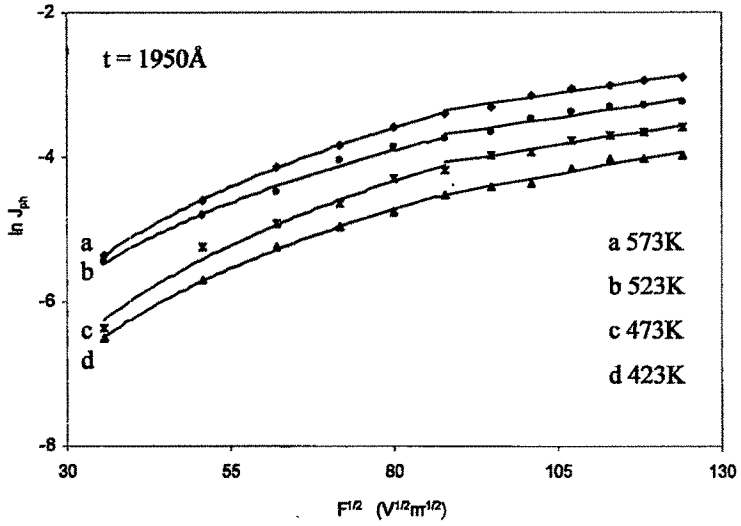

Figure 4.3(c) $\ln J_{ph}$ versus $F^{1/2}$ plots of CdSe thin films grown at different T_s, illuminated by monochromatic light (725nm).

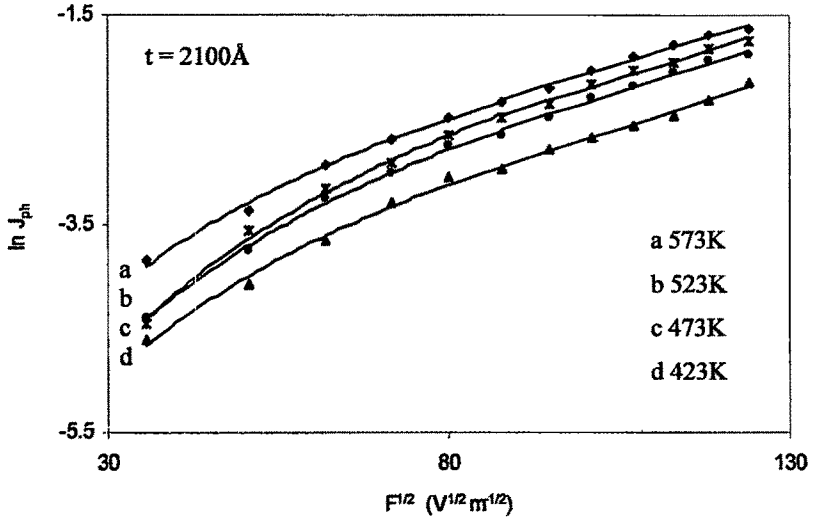

Figure 4.3(d) $\ln J_{ph}$ versus $F^{1/2}$ plots of CdSe thin films grown at different T_s, illuminated by monochromatic light (725nm).

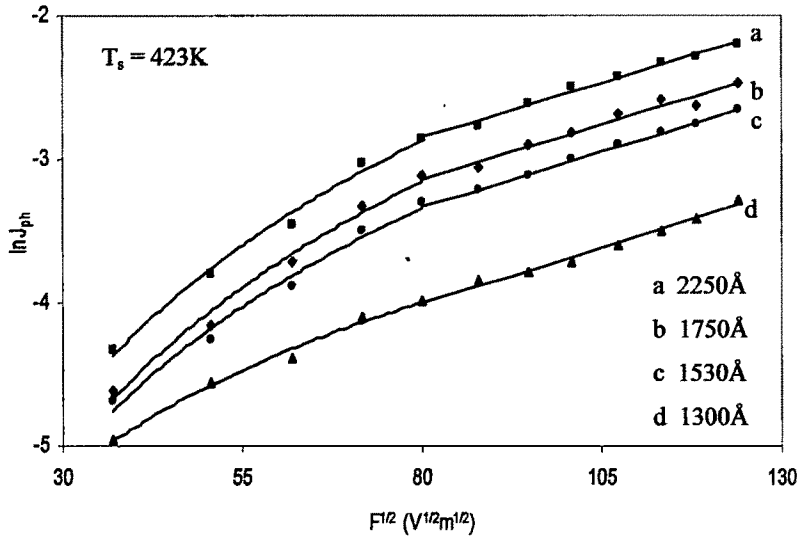

Figure 4.3(e) $\ln J_{ph}$ versus $F^{1/2}$ plots of CdSe thin films of different thickness illuminated by monochromatic light (725nm).

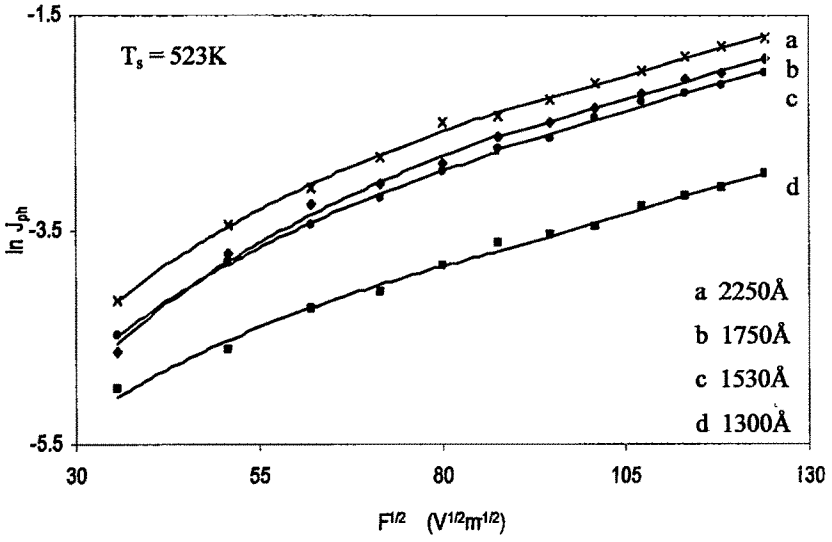

Figure 4.3(f) $\ln J_{ph}$ versus $F^{1/2}$ plots of CdSe thin films of different thickness illuminated by monochromatic light (725nm).

Table 4.1(b) Calculated values of Poole-Frenkel coefficients (β_{PF}) in 10^4 eV $V^{-1/2}$ $m^{1/2}$ unit for CdSe thin films of different thickness and grown at different T_s, illuminated by monochromatic light of 725nm.

Thickness (t) of CdSe films	Substrate temperature (T_s) of deposition			
	423K	473K	523K	573K
1950Å	4.243	3.674	3.493	3.389
2100Å	5.459	5.433	5.304	5.123
T_s of deposition	Thickness (t) of deposited films			
	1300Å	1530Å	1750Å	2250Å
423K	4.010	3.984	3.933	3.933
523K	5.289	5.226	5.175	5.149

These values of experimental β_{PF} are higher than those predicted theoretically which suggest the existence of localized electric fields within the films having values higher than mean field F = V/d. Such localized high fields may be present as a result of number of different effects; band bending in the region of the contacts due to the difference in work function between the metal and semiconductor is one possibility, while the different localized environments of individual trapping centers in the grain boundary regions of the film are unlikely to result in an exactly linear variation in potential on a microscopic scale and thus in a spatially constant electric field.

4.5 Contribution of grain boundary defects

Wide ranging technological importance of semiconductor thin films demands for a better knowledge of the defect contributions to the optoelectronic properties. Various factors like presence of external impurities, film stochiometry, substrate temperature, deposition environment etc generally determine the concentrations of various defects /31/.

Polycrystalline semiconductor thin films are made up of haphazardly oriented large number of crystallites connected by grain boundaries. The conduction mechanism

in these type of films are basically controlled by the inter crystallite grain boundaries. Thus they are the determining factors regarding the quality of various devices made on them /32/.

The various physical properties of thin films change when the nature and the temperature of the substrate, thickness or other growing parameters are altered. The variation of micro structural parameters viz crystallite stacking, rms strain, dislocation density and the stacking fault probability depends on the thickness of the film /1/. As mentioned earlier the substrate temperature during the deposition of thin film has a direct effect on the grain size, which in turn controls the grain boundary potential barrier.

4.5.1 Photocurrent versus light intensity characteristics

Photocurrents due to white light as well as different monochromatic light bear some power law dependence on the intensity of illumination, Φ which can be expressed as /34/

$$I_{ph} \propto \Phi^{\gamma} \tag{4.14}$$

where $I_{ph} = I_L - I_D$. The value of the exponent γ generally depends on the basic nature of the photoconducting medium. Exponent γ under different ambient conditions can be obtained from the slope in the plot of $\ln I_{ph}$ vs $\ln\Phi$. Some such plots are depicted in the Figs 4.4(a to h) for different CdSe thin films under monochromatic as well as white light illuminations. From the plots the values of γ are found to be in the range from 0.4 to 0.7.

It is observed that for the same film the value of γ in case of monochromatic illumination of 725nm is a little higher than that of the corresponding values for other illuminations. From the spectral response studies presented in chapter V it is found that in case of CdSe thin films the absorption corresponding to the illuminations of 725nm light is maximum. This wavelength may be regarded as optical absorption edge wavelength /33, 34/ and higher values of γ for 725 nm light is due to maximum generation rate of the photogenerated carriers. For white as well as for other illuminations values of γ remain nearly invariant for different applied bias. This implies that the transit time for photo generated carriers don't have any significant variations within the range of applied bias.

The values of exponent γ in CdSe thin films under the various experimental conditions are found to be clearly less than unity. This observation indicates that bimolecular recombination processes predominant in the photoconductivity mechanism of these films /35/. It is therefore evident that in these films various defects states are present which control the photoconductivity. These defects are essentially localized in the grain boundaries and the surfaces.

Every photosensitive material has its own characteristic pattern of absorption of incident light radiation at its surface and also within its volume. The difference between surface and volume recombinations may be understood in terms of differences in steady state photoconductivity excited by surface absorption ($h\nu < E_g$) or volume absorbed ($h\nu < E_g$) radiations /36/.

The exponent γ in relation (4.14) determines whether the recombination process is monomolecular or bimolecular which may be distinguished by the following simple relation /37/

$$g = C_n(\Delta n^2 + 2\, n_o \Delta n) \qquad (4.15)$$

where g is the generation rate, C_n is the capture coefficient, n_o is the density of thermally generated carriers and Δn is the excess carrier density. For bimolecular recombination process where $\Delta n >> n_o$, the relation (4.15) reduces to

$$\Delta n = (g/C_n)^{1/2} \propto \Phi^{1/2} \qquad (4.16)$$

which indicates that the photocurrent should be proportional to the square root of intensity of illuminations. In case of the present experimental films, as the average value of γ lies between 0.4 and 0.7, so bimolecular recombination process predominates in these films. Similar mechanism of bimolecular recombination under monochromatic illumination has also been observed by other workers /35/.

It is to be noted that both bulk as well as CdSe thin films have consistently been reported to possess n type conductivity. Both excess Cd and Se vacancies become electron donor sites which effectively act as electron trap centers. The trapping centers act as the recombination centers under illuminations. The photo generated free electron density may be expected to be greater than the trapped electrons and hence bimolecular recombination predominates in these films.

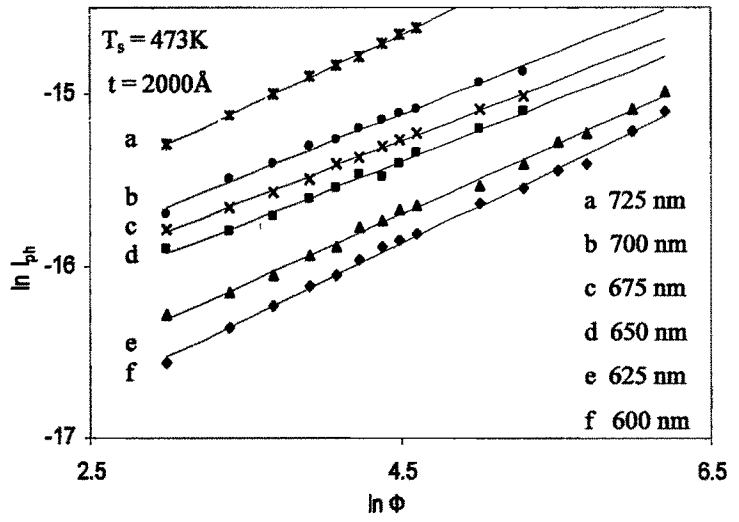

Figure 4.4(a) $\ln I_{ph}$ versus Φ plots of a CdSe thin film illuminated by different monochromatic lights.

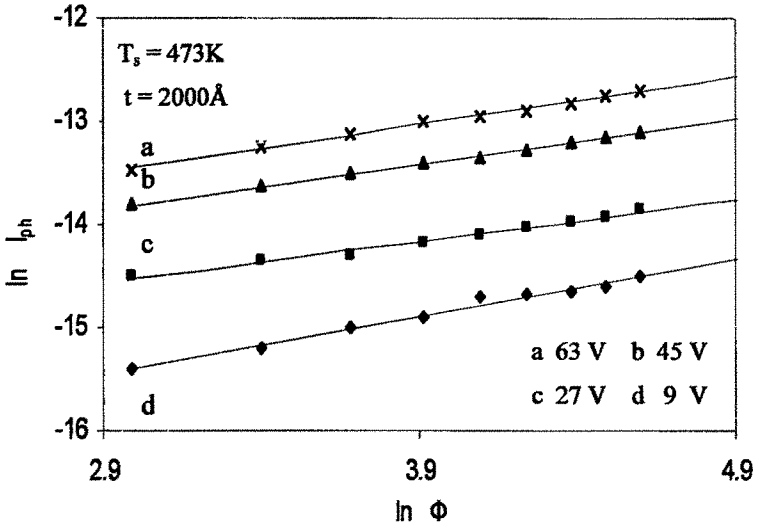

Figure 4.4(b) $\ln I_{ph}$ versus Φ plots of a CdSe thin film at different applied bias voltages and illuminated by monochromatic light (725nm).

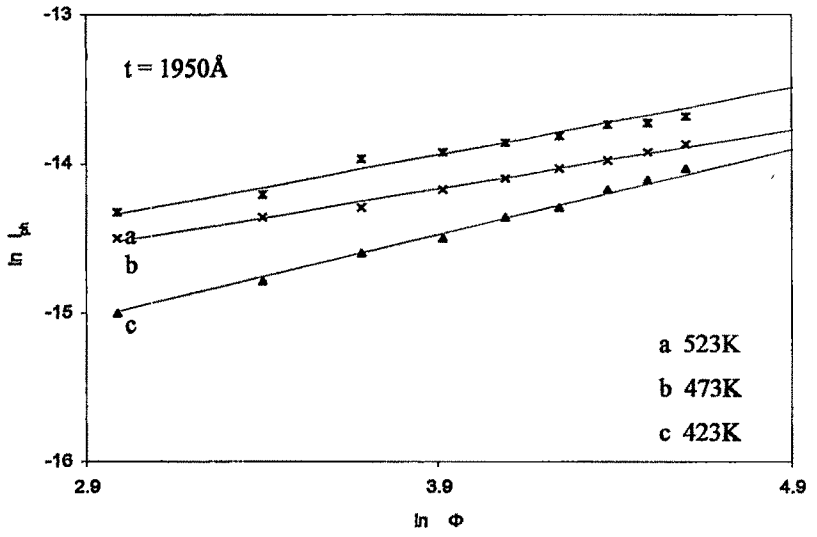

Figure 4.4(c) $\ln I_{ph}$ versus Φ plots of CdSe thin films grown at different T_s and illuminated by monochromatic light (725nm).

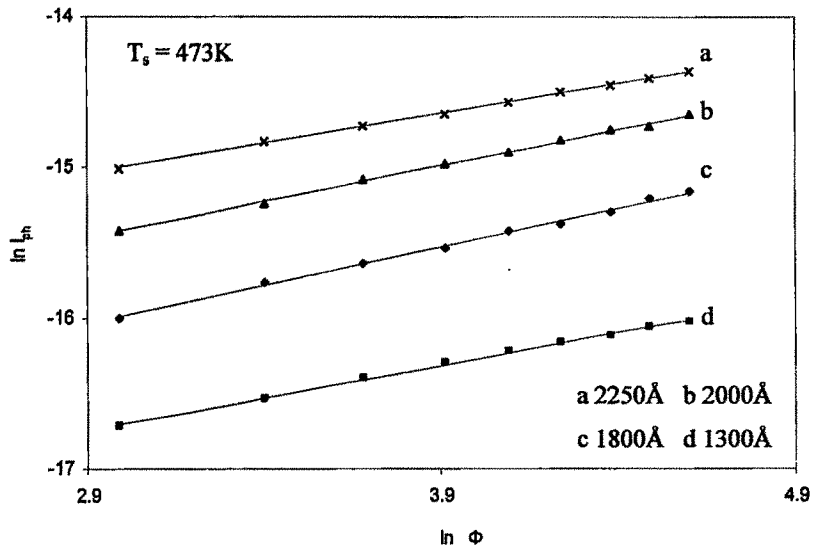

Figure 4.4(d) $\ln I_{ph}$ versus Φ plots of CdSe thin films of different thickness and illuminated by monochromatic light (725nm).

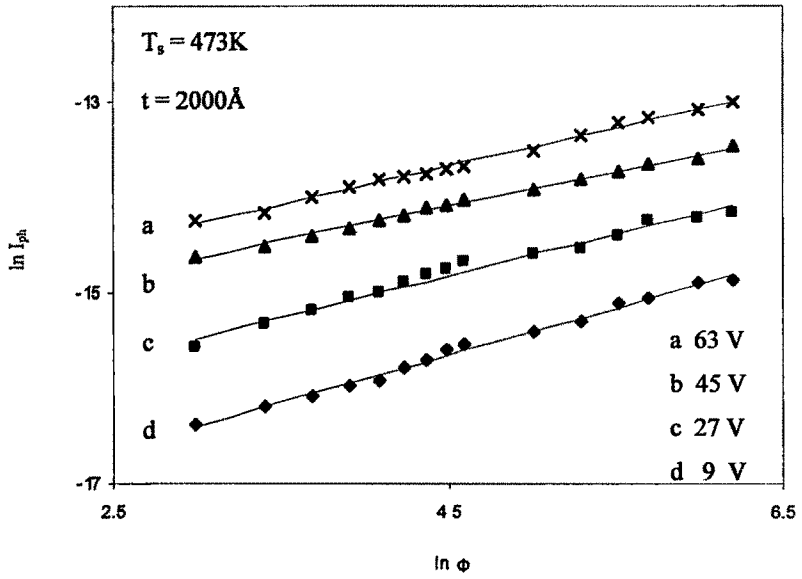

Figure 4.4(e) lnI_{ph} versus Φ plots of a CdSe thin film at different applied bias voltages and illuminated by white light.

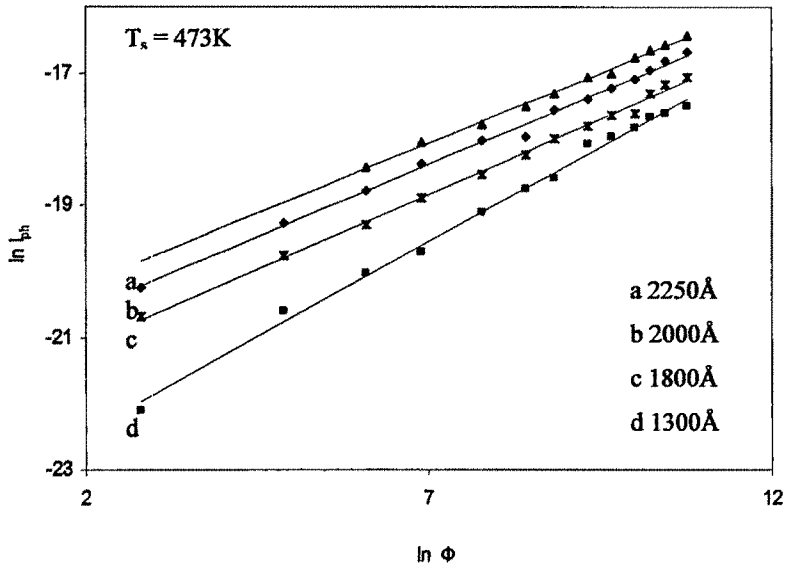

Figure 4.4(f) lnI_{ph} versus Φ plots of CdSe thin films of different thickness and illuminated by white light.

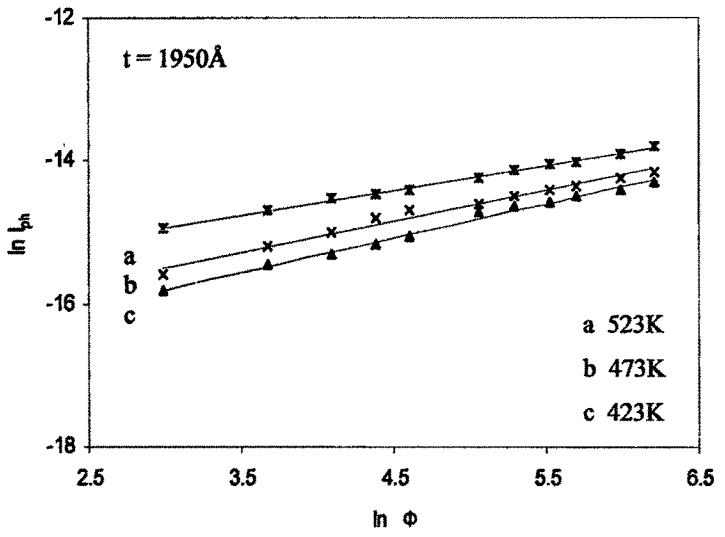

Figure 4.4(g) $\ln I_{ph}$ versus Φ plots of CdSe thin film grown at different T_s and illuminated by white light.

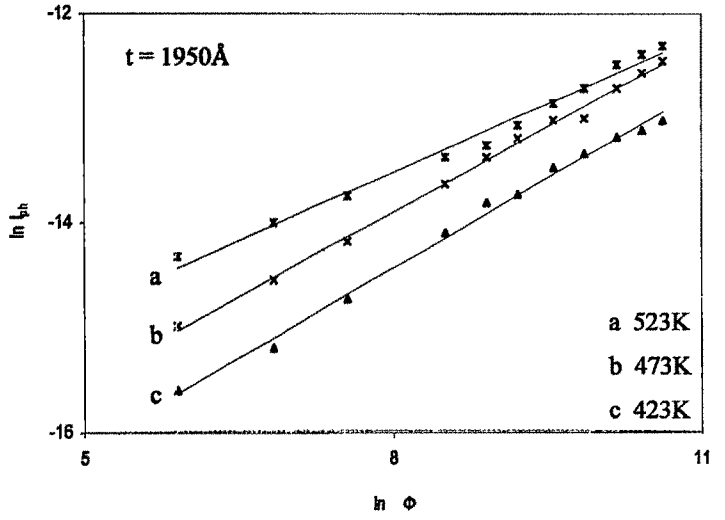

Figure 4.4(h) $\ln I_{ph}$ versus Φ plots of CdSe thin film grown at different T_s and illuminated by white light.

Rose et al. /38/ explained the variation of photocurrent with a power law of light intensity between 0.5 and 1.0 by assuming an exponential distribution of traps. With the increase of light intensity more and more trapping states are converted into recombination states. This happens because of upward movement of steady state Fermi level through the trap levels towards the conduction band. With the increase in the density of the recombination states for electrons, free carrier life time decreases. According to Rose, this decrease in life time is indicated by an exponential, γ, having value less than unity.

4.6. Temperature dependence of conductivity

The variation of dark conductivity, σ_D, and conductivity under illumination, σ_L, of CdSe thin films (different t & T_s) with ambient temperature in the range from room temperature to 500K were studied. Both dark and current under illumination (I_D, I_L) were found to be increase exponentially with temperature for all the films. Dependence of ln σ_D (or ln σ_L) are plotted as a function of temperature 1000/T, for the said films. The plots are shown in the Figs 4.5(a to f). From the plots it is observed that, the CdSe thin films are characterized by double activation regions in the covered range of temperature.

The observed activation energies (ΔE), calculated from the respective slopes of the plots, are systematically presented in the Table 4.2(a) and Table 4.2(b). The activation energies under illumination are found to decrease with illumination level. Activation energies both in dark and under illumination decrease with T_s. The reduction in activation energies may be explained by the grain boundary effect in polycrystalline films as suggested by Petritz /4/. Such variation is also reported by other workers /39/.

Grain boundaries in polycrystalline films contain a large number of defects which results in the formation of energy states within the band gap. They act as effective carrier traps and after trapping carriers, the states become charged and there by give rise to some potential barriers. The barriers localized at the grain boundaries modulate the conductivity in the films. The current carriers have to pass through a number of such grain boundary potential barriers.

For uniform grain boundary structure with identical barrier, the conductivity may be expressed as

$$\sigma = nq\mu^*$$

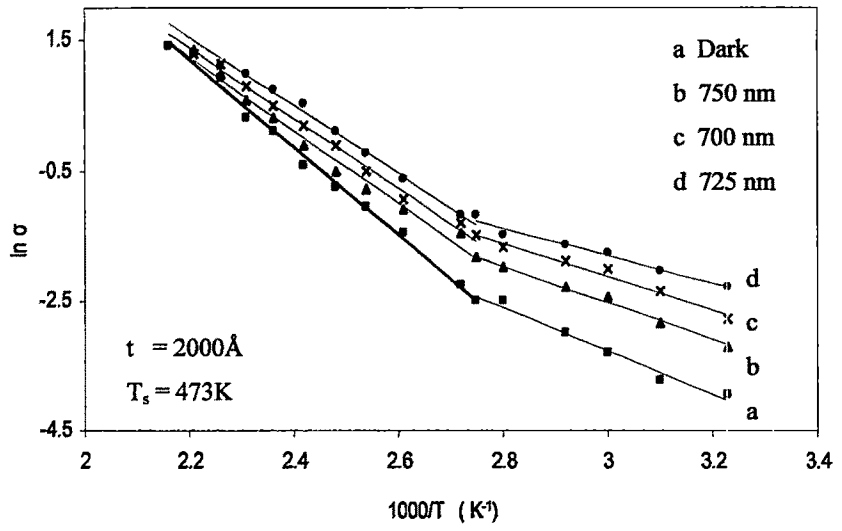

Figure 4.5(a) $\ln\sigma_D$ ($\ln\sigma_L$) versus 1000/T plots of a CdSe thin film at dark and under different monochromatic illuminations.

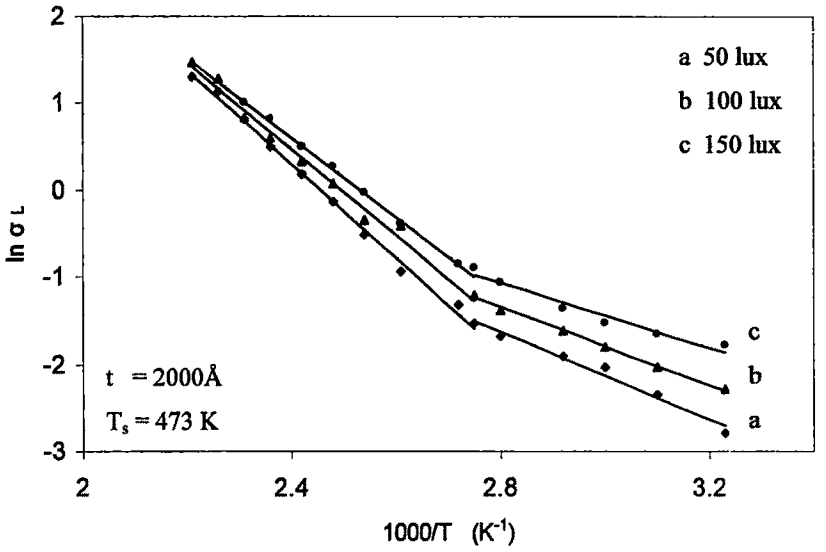

Figure 4.5(b) $\ln\sigma_L$ versus 1000/T plots of a CdSe thin film illuminated by monochromatic light (725nm) of different intensities.

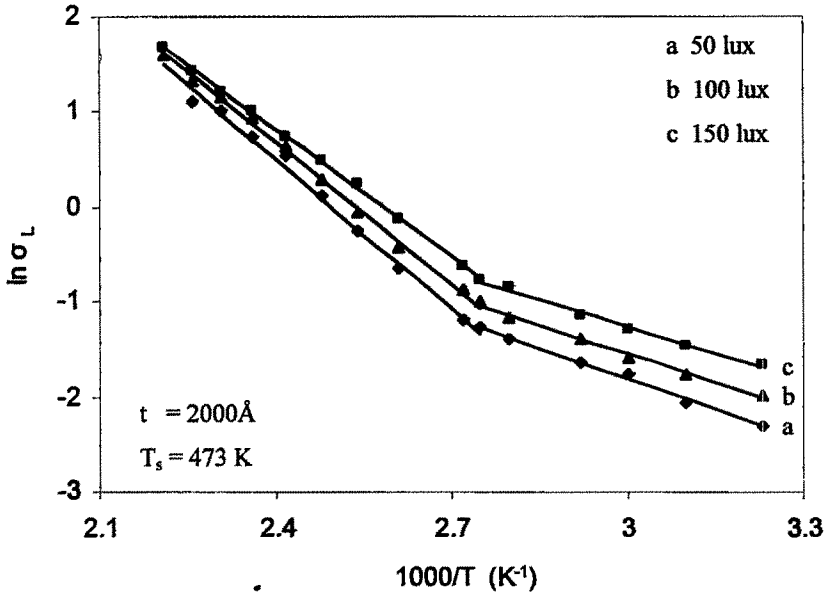

Figure 4.5(c) $\ln\sigma_L$ versus 1000/T plots of a CdSe thin film illuminated by monochromatic light (700nm) of different intensities.

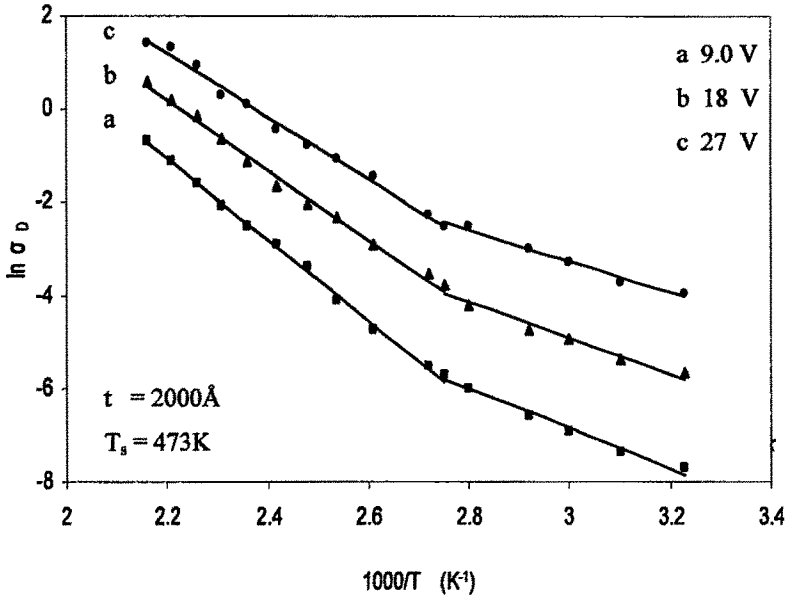

Figure 4.5(d) $\ln\sigma_D$ versus 1000/T plots of a CdSe thin film at different applied bias voltages.

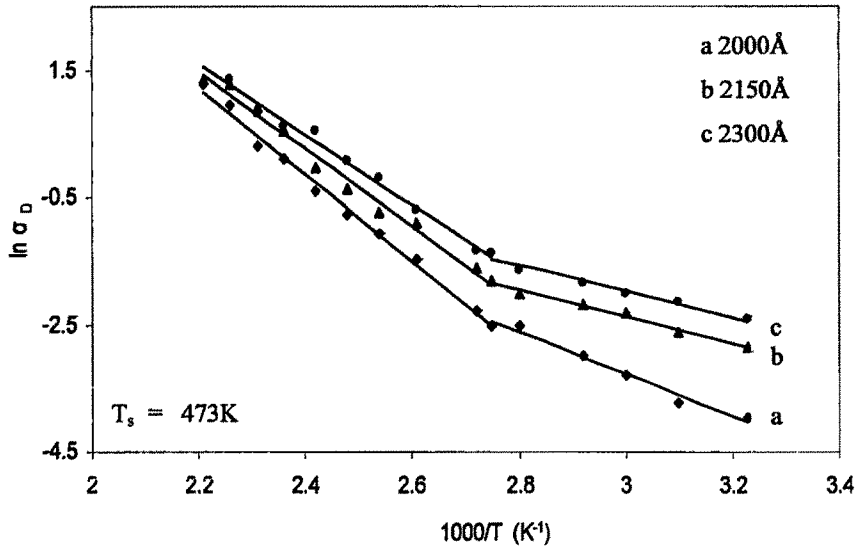

Figure 4.5(e) $\ln\sigma_D$ versus 1000/T plots of CdSe thin films having different thickness.

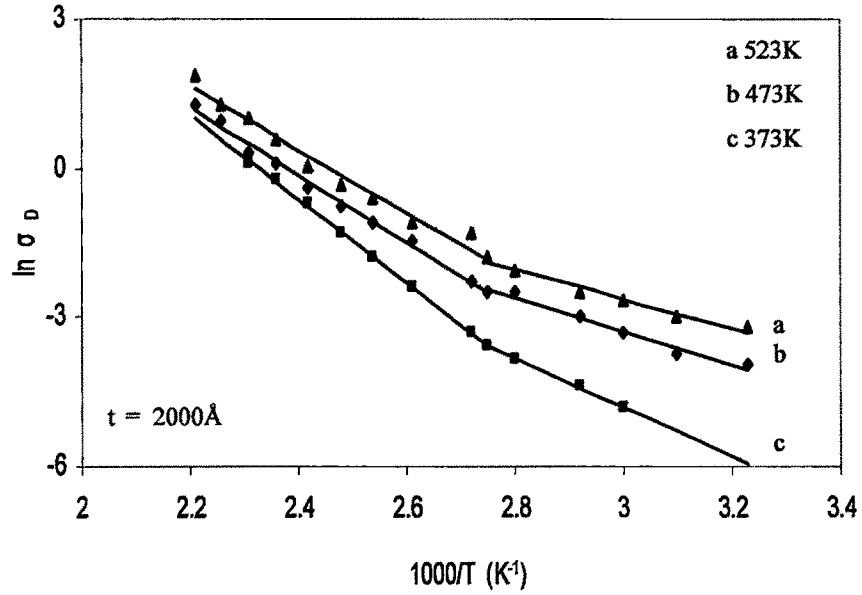

Figure 4.5(f) $\ln\sigma$ versus 1000/T plots of CdSe thin films grown at different T_s.

$$= nq\mu_o \exp(-q\Phi_b / kT_o) \quad (4.17)$$

where n is the majority carrier concentration and μ^* is the effective mobility of carrier which is expressed by equation (4.12).

Considering only one type of carrier dominating the conduction process, the carrier density may be written as

$$n = 2(2n_d)^{1/2}(2\pi m_e^* kT/h^2)^{3/4}\exp(-\Delta E/kT) \quad (4.18)$$

So the dark conductivity

$$\sigma_D = nq\mu^* = \sigma_o \exp(-\Delta E/kT) \quad (4.19)$$

where $$\sigma_o = 2q\mu_o (2n_d)^{1/2} (2\pi m_e^* kT/h^2)^{3/4}\exp(-q\Phi_D/kT_o)$$

where ΔE is the donor or acceptor level activation energy, Φ_D is the barrier height in dark, which is greater than the same under illumination i.e. Φ_L.

σ_D increases primarily due to increase in thermally generated carriers, thus the activation process is dominated by the term $\exp(-\Delta E / kT)$ in equation (4.19). In this case, the effective barrier modulation is small. Therefore, with respect to the carrier activation process, determined by the temperature dependent exponential term $\exp(-\Delta E / kT)$, the mobility term may be taken to be effectively independent of temperature /40/.

Now when the film is illuminated by white or monochromatic light the photoconductivity increases over the dark values. The total conductivity under external illumination may be expressed as

$$\sigma_L = nq\mu^* = \sigma_o \exp(-\Delta E/kT) \quad (4.20)$$

where $$\sigma_o = 2q\mu_o (2\pi kT/h^2)^{3/2}(m_e^* m_h^*)^{3/4}\exp(-q\Phi_L/kT_o)$$

Thus the change in conductivity with temperature may be either due change in carrier density or mobility or of both of these parameters. It is therefore, clear that the evaluated activation energy is the total conductivity activation energy. The activation energy decreases under illumination mainly through reduction in Φ_L and the conductivity increases over its dark value. Since the carrier activation energy ΔE is nearly independent of temperature in the respective temperature regions, from a calculation of the difference

of dark activation and photo activation energies mobility activation energy can be evaluated.

The grain boundary potential barrier, Φ_b, can be expressed as /2, 6/

$$\Phi_b = (Q_t - \Delta P_t) / 8\varepsilon\varepsilon_o\Delta n \qquad (4.21)$$

where Δn is the photo generated carrier density, which is greater than the density of majority carrier traps, Q_t localized at the grain boundaries, ε and ε_o are the dielectric constants of the material of the film and free space respectively. ΔP_t is the density of trapped minority carriers under illumination in the depletion region. It may be noted that ΔP_t increases with the illumination level.

Of the photo generated carriers, which are in excess to the thermal equilibrium carriers at any temperature, a part is responsible for enhancement of conductivity (photoconductivity) and the other part goes to neutralize some fraction of the corresponding localized charges in the depletion region between the grains. This results in the reduction in the grain boundary potential barrier Φ_b. Thus one gets $\Phi_D > \Phi_L$ where, as already mentioned, Φ_D and Φ_L are the grain boundary potential barriers under dark and under illumination respectively. Due to reduction of barrier height the effective mobility μ^* under illumination gets enhanced. This is known as the barrier or mobility modulation process.

As a result of this mobility activation, due to illumination, the current density under illumination gets enhanced over the corresponding dark values. From equation (4.12) the effective mobility under dark and illumination can be written as

$$\mu_D^* = \mu_o \exp(-q\Phi_D/kT_o) \qquad (4.22a)$$

$$\mu_L^* = \mu_o \exp(-q\Phi_L/kT_o) \qquad (4.22b)$$

The change in mobility due to illumination is given by

$$\Delta\mu^* = \mu_L^* - \mu_D^* \qquad (4.23)$$

Since $\Phi_D > \Phi_L$, $\mu_D^* < \mu_L^*$, $\Delta\mu^*$ is positive.

Table 4.2(a) Activation energies in dark (ΔE_D), under illumination (ΔE_L) and mobility activation (ΔE_μ) energies for a CdSe thin film (t = 2000Å, T_s = 473K) in temperature regions R-I (360 to 453K) and R-II (300 to 360K).

Φ lux	ΔE (eV)	Dark ΔE_D (eV)		ΔE_L & ΔE_μ (eV) under monochromatic light of λ					
				750 nm		700 nm		725 nm	
		R-I	R-II	R-I	R-II	R-I	R-II	R-I	R-II
40	ΔE_D, ΔE_L	0.584	0.288	0.489	0.244	0.467	0.219	0.453	0.185
	ΔE_μ	-	-	0.094	0.043	0.117	0.068	0.131	0.103
λ nm	ΔE (eV)	Dark ΔE_D (eV)		ΔE_L & ΔE_μ (eV) under monochromatic light of Φ					
				50 lux		100 lux		150 lux	
700	ΔE_D, ΔE_L	0.584	0.288	0.467	0.217	0.430	0.192	0.397	0.160
	ΔE_μ	-	-	0.116	0.071	0.154	0.095	0.186	0.112
725	ΔE_D, ΔE_L	0.584	0.288	0.453	0.185	0.431	0.173	0.386	0.164
	ΔE_μ	-	-	0.131	0.103	0.153	0.110	0.198	0.124

Table 4.2(b) Dark activation energies (ΔE_D) in eV of CdSe thin films of different thickness and grown at different T_s in temperature regions R-I (360 to 453K) and R-II (300 to 360K).

t , T_s and applied bias of the films	Applied bias voltage					
	9V		18V		27V	
	R-I	R-II	R-I	R-II	R-I	R-II
t=2000Å,T_s=473K	0.756	0.369	0.651	0.331	0.584	0.288
Applied bias and T_s of film	Thicknesses (t) of the film					
	2000Å		2150Å		2300Å	
T_s = 473K	R-I	R-II	R-I	R-II	R-I	R-II
Bias = 27V	0.584	0.288	0.529	0.182	0.482	0.174
Applied bias and t of film	Elevated substrate temperature (T_s) of the film					
	423K		473K		523K	
t = 2000Å	R-I	R-II	R-I	R-II	R-I	R-II
Bias = 27V	0.729	0.422	0.584	0.288	0.552	0.248

At any temperature $\sigma_L > \sigma_D$ and in the $\ln\sigma$ versus 1000/T plots in the both activation regions $(\text{slope})_L < (\text{slope})_D$. The decrease in slope under illumination is due to mobility activetion process. Hence it can be obtained from the difference of $(\text{slope})_L$ and $(\text{slope})_D$.

Let ΔE_D, ΔE_L and ΔE_μ represent the activation energies in dark, under illumination and mobility activation energy respectively. It may be noted that $\Delta E_D > \Delta E_L$, in general. Hence

$$\Delta E_\mu = \Delta E_D - \Delta E_L, \text{ is a positive quantity.}$$

Calculated changes in mobility activation energies are presented in Table 4.2(a) for different illumination levels.

Present results of mobility activation energy under different illuminations in thermally evaporated CdSe thin films nearly agree with those of Barua et. al /41/. Several other workers also reported about activation energy and its reduction under illuminations in CdSe thin films /18,26,39,42-45/. The magnitudes of observed activation energy are found close to those reported values.

4.7 Correlative assessment

4.7.1 Variation of photosensitivity with temperature

The photosensitivity is defined as

$$S = I_{ph} / I_D = (I_L - I_D) / I_D \qquad (4.24)$$

where I_{ph} is the photocurrent, I_L and I_D are respectively current under illumination and current in dark, as mentioned earlier.

The variation of photosensitivity with temperature for a CdSe thin film of thickness 2000Å and deposited at T_s = 473K are depicted in Fig 4.6(a). The photosensitivity is found to be maximum for the film, at room temperature condition under different monochromatic illuminations and decreases rapidly with ambient temperature showing there by that there is an exponential like decrease of photosensitivity with ambient temperature. Similar type of observation of temperature dependence of photosensitivity was also reported by other worker /46/.

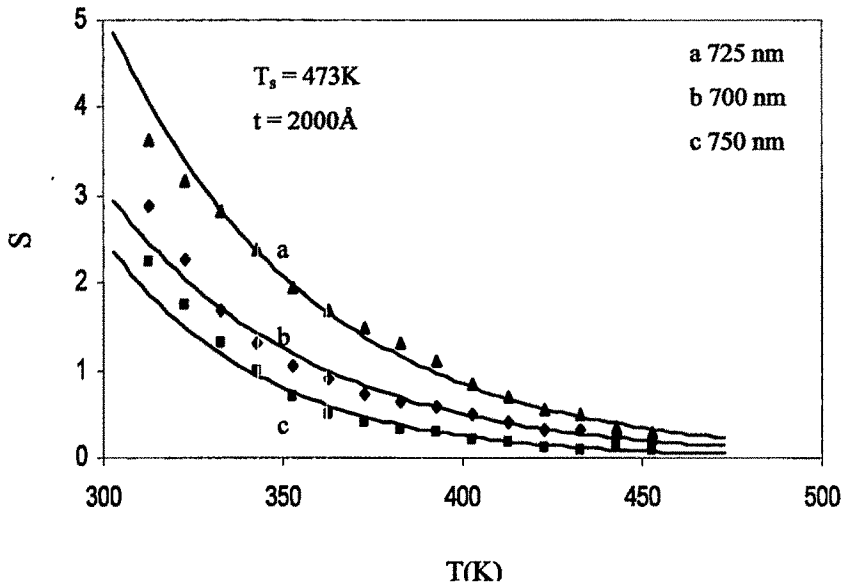

Figure 4.6(a) Variation of photosensitivity (S) with ambient temperature, T(K) under different monochromatic illuminations for a CdSe thin film (Φ = 40 lux).

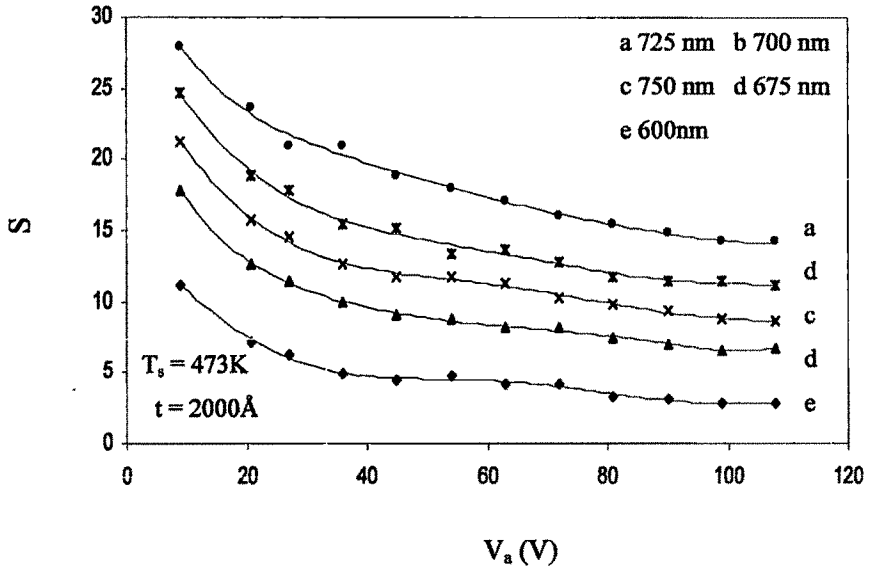

Figure 4.6(b) Variation of photosensitivity (S) with applied bias voltage, V_a (V) under different monochromatic illuminations for a CdSe thin film (Φ = 100 lux).

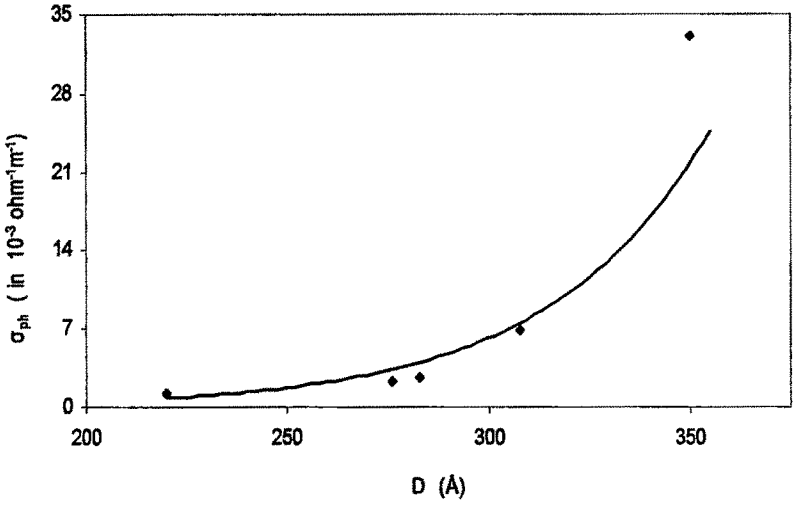

Figure 4.7(a) Variation of photoconductivity (σ_{ph}) with grain size (D) of CdSe thin films of constant t = 2000Å and grown at different elevated T_s.

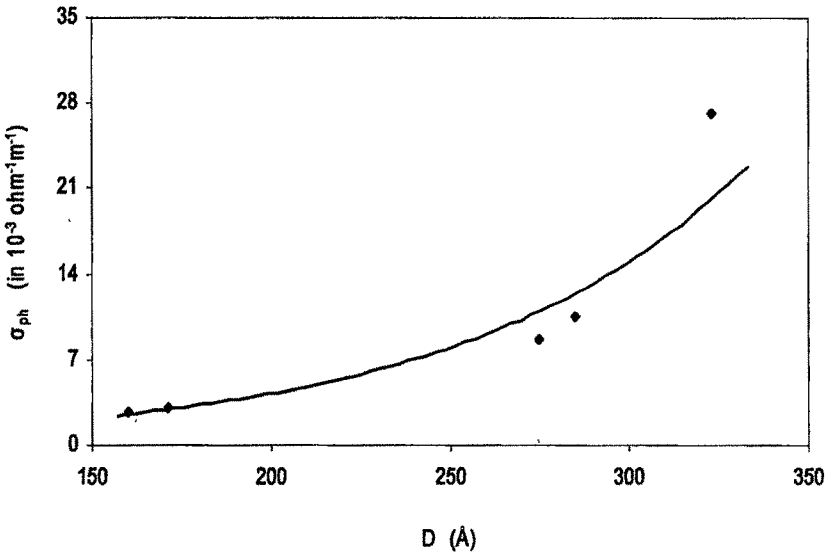

Figure 4.7(b) Variation of photoconductivity (σ_{ph}) with grain size (D) of CdSe thin films of different, t, and grown at constant elevated T_s = 473K

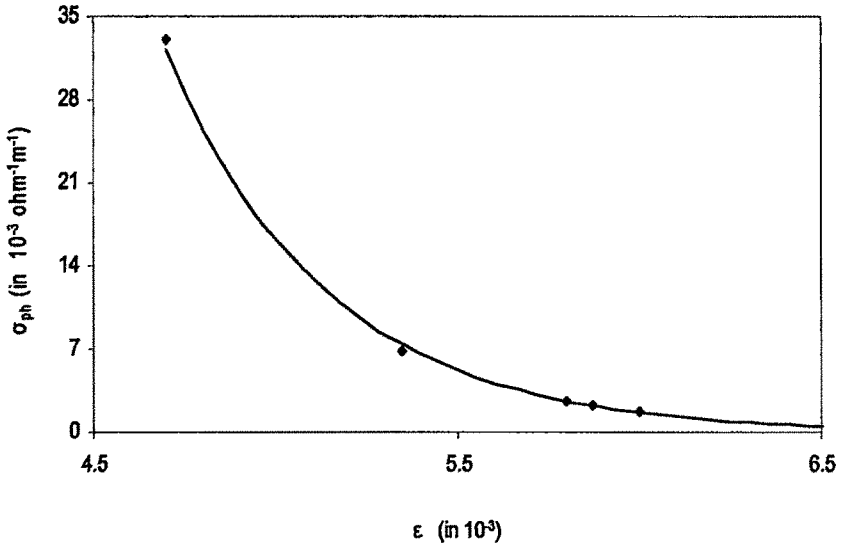

Figure 4.8(a) Variation of photoconductivity (σ_{ph}) with strain (ε) of CdSe thin films of constant t = 2000Å grown at different elevated T_s.

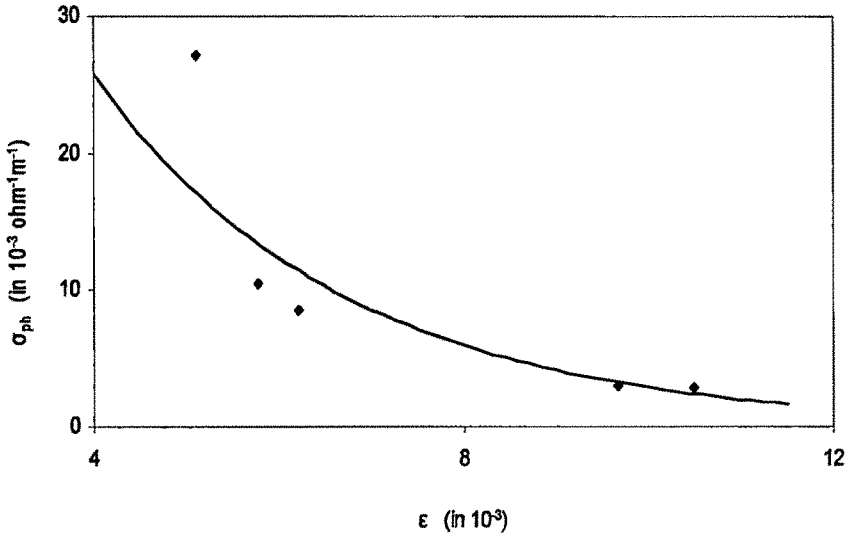

Figure 4.8(b) Variation of photoconductivity (σ_{ph}) with strain (ε) of CdSe thin films of different, t, and grown at constant elevated T_s = 473K

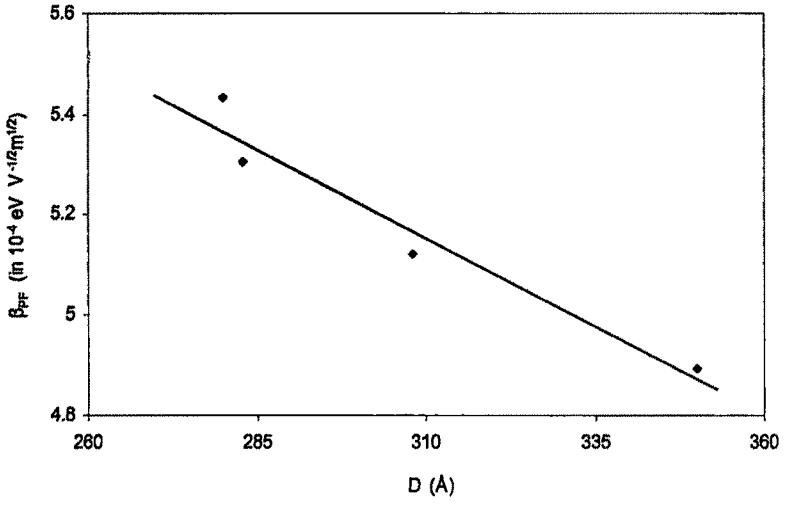

Figure 4.9(a) Variation of Poole-Frekel coefficient (β_{PF}) with grain size (D) of CdSe thin films of constant t = 2000Å and grown at different elevated T_s.

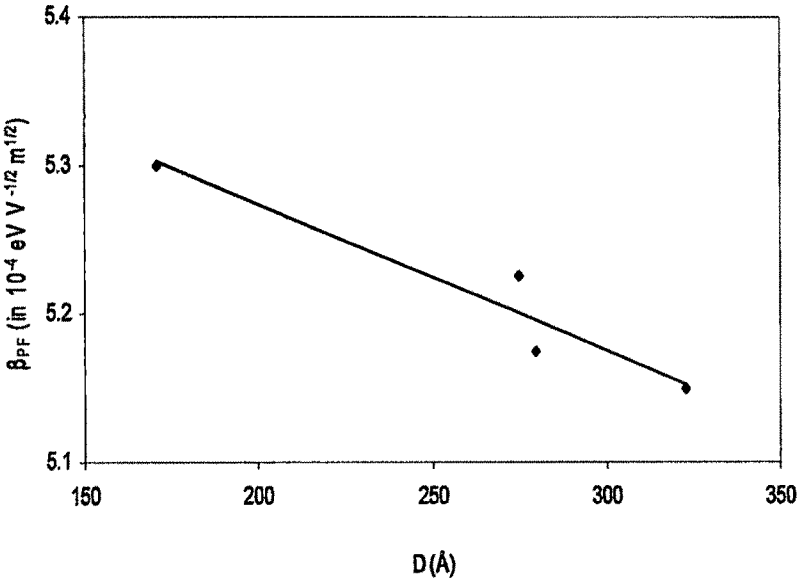

Figure 4.9(b) Variation of Poole-Frekel coefficient (β_{PF}) with grain size (D) of CdSe thin films of different, t, and grown at constant elevated T_s = 473K

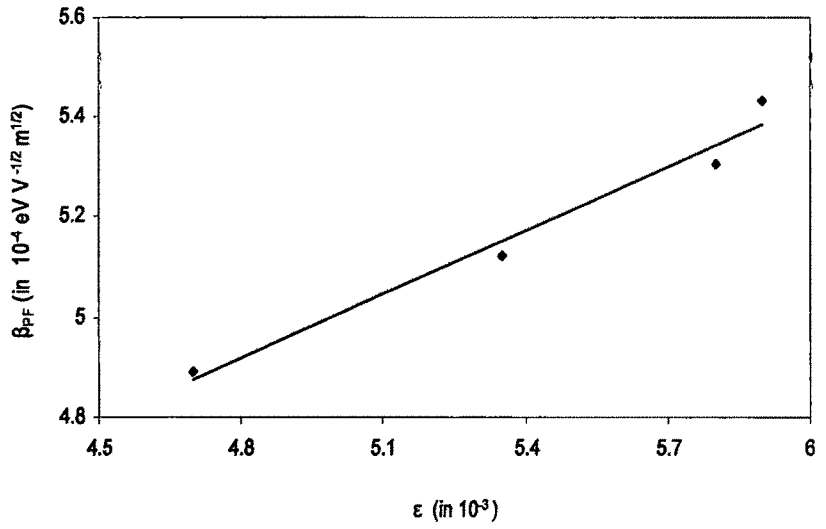

Figure 4.10(a) Variation of Poole-Frekel coefficient (β_{PF}) with strain (ε) of CdSe thin films of constant t = 2000Å and grown at different elevated T_s.

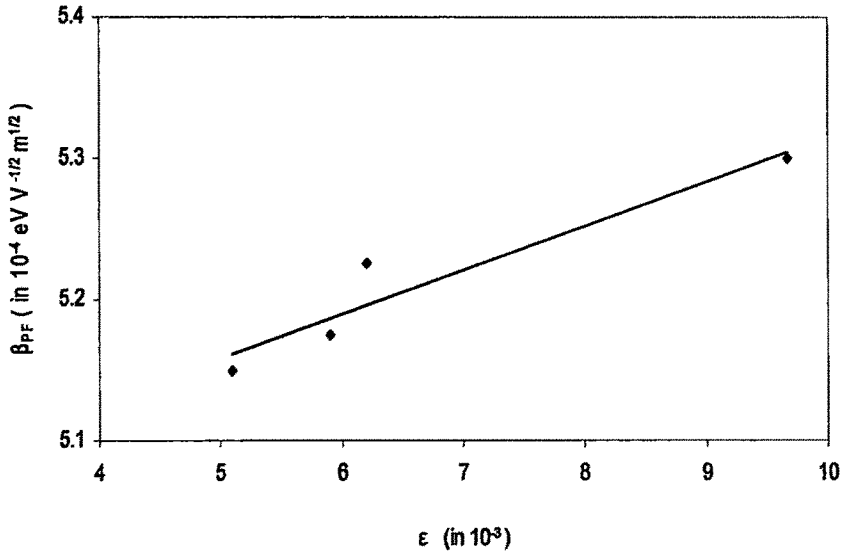

Figure 4.10(b) Variation of Poole-Frekel coefficient (β_{PF}) with strain (ε) of CdSe thin films of different, t, and grown at constant elevated T_s = 473K.

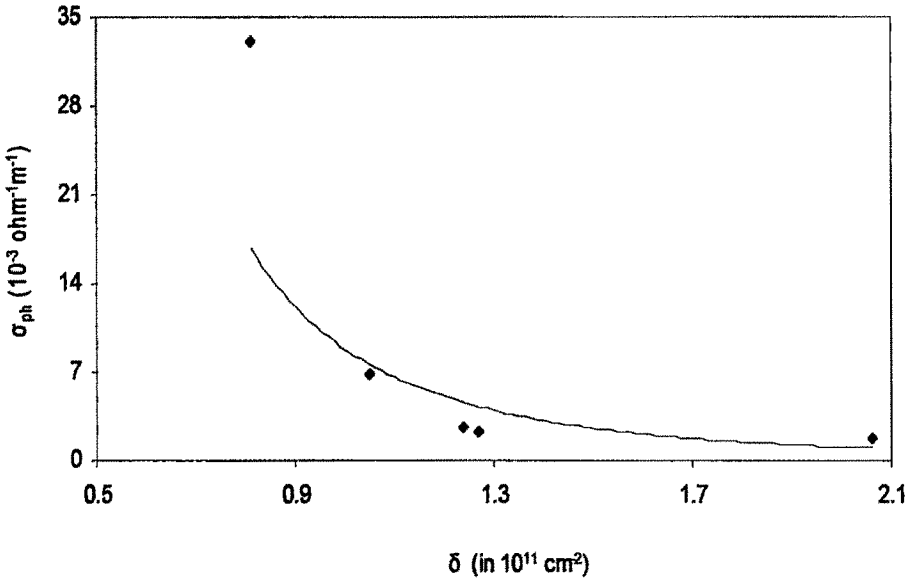

Figure 4.11(a) Variation of photoconductivity (σ_{ph}) with dislocation density (δ) of CdSe thin films of constant, t = 2000Å and grown at different elevated T_s.

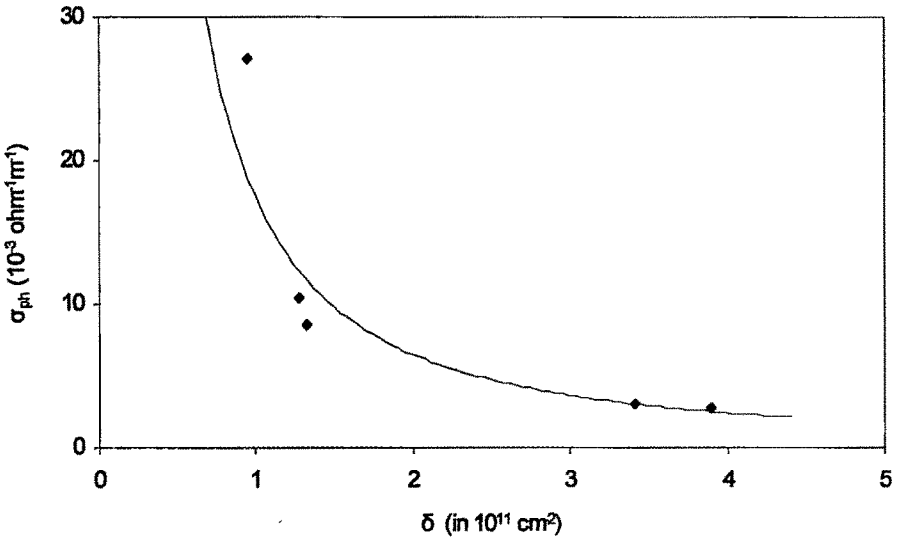

Figure 4.11(b) Variation of photoconductivity (σ_{ph}) with dislocation density (δ) of CdSe thin films of different, t, and grown at constant elevated T_s = 473K.

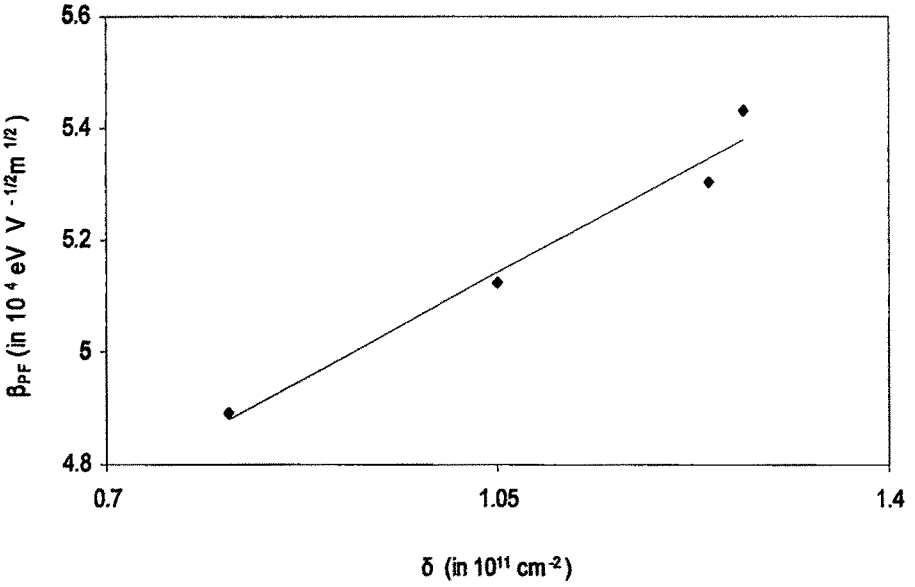

Figure 4.12(a) Variation of Poole-Frekel coefficient (β_{PF}) with dislocation density (δ) of CdSe thin films of constant t = 2000Å and grown at different elevated T_s.

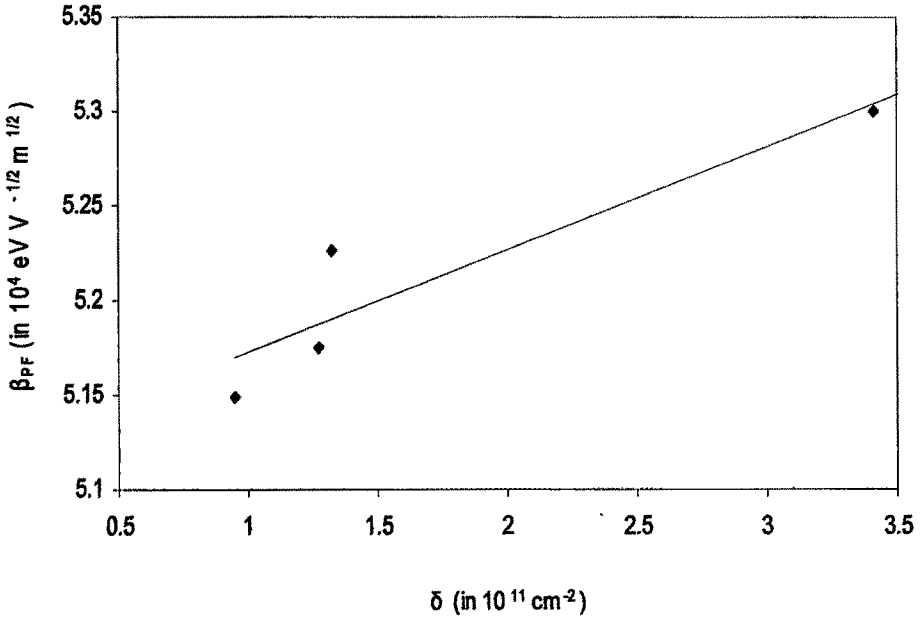

Figure 4.12(b) Variation of Poole-Frekel coefficient (β_{PF}) with dislocation density (δ) of CdSe thin films of different, t, and grown at constant elevated T_s = 473K

4.7.2 Variation of photosensitivity with bias

There is an increase of both dark as well as photocurrents of the experimental films with applied bias, when the ambient temperature is the room temperature. This is mainly due to enhancement of transit time and consequent reduction of recombination rate and probability of trapping of the carriers. The photosensitivity S, given by equation (4.24), is seen to decrease with increasing bias. This behaviour is displayed in Fig 4.6(b) for a film grown at elevated T_s under different monochromatic illuminations of constant intensity. The variation of S for different wavelength is due to corresponding impurity level contributions.

4.7.3 Photoconductivity versus grain size

In the present study the photoconductivity of CdSe thin films is found to increase rapidly with grain size in films deposited at different T_s and of different t. The Fig 4.7(a) and Fig 4.7(b) respectively show the said dependences. XRD data show that films grown at higher T_s are essentially polycrystalline with higher grain size and the photoconductivity increases with reduction of grain boundary defect states.

4.7.4 Photoconductivity versus strain

As is seen in Fig 4.7(a) and Fig 4.7(b) that there is a rapid increase of photoconductivity with grain size (D) and there is a decreasing behaviour of strain with D (Fig. 3.10) which is mainly related with the temperature of deposition. As already mentioned, crystallinity of the films is found to improve with T_s. From the plots of photoconductivity versus strain, as depicted in Fig 4.8(a) and Fig 4.8(b), it is observed that there is a decreasing tendency of photoconductivity with strain.

4.7.5 Poole-Frenkel coefficient versus grain size

From the present analysis it is found that I_{ph} increases linearly with bias in low field and exponentially in high field region. The photoconductivity of the films is dependent on the grain sizes as observed from Fig 4.7(a) and Fig 4.7(b). The presented results include the variation of β_{PF} with grain size of films of different thickness and

deposited at different T_s. It has been observed that β_{PF} has a linear relationship with the grain size with a negative slope, as shown in the Fig 4.9(a) and Fig 4.9(b).

4.7.6 Poole-Frenkel coefficient versus strain

It is already observed in Chapter III that grain size in a thermally evaporated CdSe thin film increases with T_s. From the plots (Fig. 3.10) of strain versus grain size, it has been found that in the studied thin films there is a tendency of decrease of strain with grain size. Plots of Poole-Frenkel coefficient versus strain depicted in Fig. 4.10(a) and Fig. 4.10(b) shows that the coefficient increases with strain.

4.7.7 Photoconductivity versus dislocation density

In the polycrystalline samples dislocated atoms occupy the regions near the grain boundaries. The effect due to the presence of dislocated atoms or molecules near grain boundary on the electronic structure and optical properties of polycrystalline semiconductor is mainly determined by (a) crystal structure distortions, (b) the presence of mechanical stresses due to structural defects, (c) internal electric fields arising as a result of screening of the charge near the grain boundary /47/. Fig 4.11(a) and Fig 4.11(b) show the plots of photoconductivity versus average dislocation density of CdSe thin films of constant, t, deposited at different T_s and films of different, t, grown at constant T_s respectively. It is found that the photoconductivity of the films decreases exponentially with the dislocation density. Therefore it can be concluded that the increase in the number of dislocation enhance the contribution of defects which in turn reduce the photoconductivity films.

4.7.8 Poole-Frenkel coefficient versus dislocation density

It is observed from Fig 4.9(a) and Fig 4.9(b) that Poole-Frenkel coefficient (β_{PF}) decreases gradually with the increase of grain sizes, and dislocation density has an inverse square variation with grain sizes. Fig 4.12(a) and Fig 4.12(b) show the plots of β_{PF} versus dislocation density of CdSe thin films of constant, t, deposited at different T_s and films of different, t, grown at constant T_s respectively. For both the cases a linear variation has been observed between β_{PF} and dislocation density.

4.8 Conclusions

For the present study of optoelectronic properties in thermally evaporated CdSe thin films, films having different thickness and deposited at different elevated T_s were used. Dark conductivity of such films yields ohmic contacts with thermally evaporated aluminium electrodes. For the observations taken at various ambient temperatures also the ohmic nature of contact prevails.

Vacuum evaporated 'as-grown' films of CdSe at room temperature are not photosensitive. These films show very poor photosensitivity in comparison to the films deposited at higher T_s even after thermal annealing. Thermally evaporated films of CdSe show defect controlled photoconductivity. The photocurrent varies sublinearly with light intensity (white as well as monochromatic) which indicates the predominance of bimolecular recombination process in these films. This particular nature is independent of film thickness, T_s and applied bias. For a film of constant thickness deposited at elevated T_s there is a decrease in photosensitivity with the increase in applied bias. The photo sensitivities of the films were also found to decrease strongly with ambient temperatures.

The resistivity of CdSe thin film samples deposited by the technique of thermal evaporation in vacuum depends on several parameters like thickness of the film, T_s of deposition, rate of deposition, heat treatment in vacuum etc. The decrease in the resistivity of the films prepared at higher T_s and on thermal annealing could be associated with the recrystallization effect of the film material, mainly due to the increase of effective mobility. Thus the T_s of the grown films play a prominent role in the photoconduction mechanism. Increase of T_s results in the subsequent increase in photosensitivity. Annealing of the CdSe films at elevated temperature changes the level of photoconductivity.

From the plots of I_{ph} vs V_a of CdSe thin films it is observed that no space charge injection mechanism prevailing in the sample and the photoconductivity phenomenon is governed by Poole-Frenkel mechanism. The experimental values of β_{PF} obtained from the Poole-Frenkel expression are higher than the corresponding theoretical values.

Temperature dependence characteristics have been observed in CdSe thin films for both photo and dark current. The evaluated values of activation energies for these

CdSe thin films vary in the range from 0.49 to 0.38 eV and 0.24 to 0.16 eV under illumination of different intensity for the considered higher and lower temperature regions respectively. The activation energies in higher temperature regions are higher than their corresponding values in the lower temperature regions. In this case the band edge value for CdSe is seen to be higher than the theoretical one. This may be due to some modified transition probabilities.

The activation energies in CdSe thin films were found to decrease with illumination levels. This is attributed to reduction of grain boundary barrier heights by photo generated carriers. The observed decrease of activation energies with temperature of deposition is a consequence of improvement of crystallinity with T_s. The same reason can be attributed to the observed enhancement in photoconductivity with T_s. The values of activation energies were found to decrease with thickness also. Photoconductivities of CdSe thin films are observed to be some strong function of film thickness.

4.9 References

1. S. Saha, U. Pal, B. K. Samantary, A. K. Choudhary and H. D. Banerjee; *Thin Solid Films*, 164, 1988, 88.
2. K.C. Sarmah and H. L. Das; *Thin Solid Films*, 198, 1991, 29.
3. A. Rose, *Phys. Rev.* 97, 322, 1955.
4. R. L. Petritz, *Phys. Rev.*; 104(6), 1956, 1508.
5. J. M. Pawlikowski, *Thin Solid films*, 190, 1990, 39.
6. J. Y. W. Seto. *J. Appl. Physics*, 46, 1975, 5247.
7. S. C. Bhatnagar and S. R. Verma, *Indian J. of Pure & Appl. Phys.* 32, 1994, 375.
8. J. Dutta, D. Bhattacharyya, S. Chaudhuri and A. K. Pal.; *Solar Energy Materials and Solar Cells*, 36, 1995, 357.
9. R. E. Thun in G. Hass (Ed.), *Physics of Thin Films*, Vol. 1, Academic Press, New York, 1963, P. 212.
10. P. S. Vincett, W. A. Barlow and G. G. Roberts, *J. Appl. Phys.;* 48(9), 1977, 3800.
11. J. C. Anderson, *Advances in Physics*, 19(79), 1970, 326.
12. A. F. Mayadas and M. Shatzkes. *Phys. Rev.* B1, 1970, P 302.

13. J. Worton and M. J. Powell, *Rep. Prog. Phys.* 43, 1980, 1269.
14. R. H. Bube, *Photoconductivity in Solids*, Wiley, N. Y. 1963, P 82.
15. V. Snejdar and J. Jerhot, *Thin Solid Films*, 37, 1976, 303.
16. S. A. Mahmoud, A. Ashour and E. A. Badawi; *Applied Surface Science*, 253, 2006, 2969-2972.
17. A. O. Oduor and R. D. Gould, *Thin Solid Films*; 270, 1995, 387-390.
18. M. Buragohain and K. Barua, *Thin Solid Films*, 99, 1983, L1-L4.
19. A. Mondal, A. Dhar, S. Chaudhari and A. K. Pal, *J. Mat. Sc.*, 25, 1990, 2221.
20. D. Nesheva, S. Reynolds, Z. Aneva, C. Main and Z. Levi, *J. Optoele. Adv. Mat.*; 7(1), 2005, 517-520.
21. M.B. Winn and L.E. Lyons, *Aust. J. Chem*, 38, 1985, 841.
22. H. Okimura and Y. Sakai, *Jap. J. Appl. Phys*, 7(7), 1968, 7341.
23. L. Ion, S. Antohe, M. Popescu, F. Scarlat, F. Sava and F. Ionescu, *J. Optoele. Adv. Mat.*, 6(1), 2004, 113-119.
24. F. Raoult, B. Fortin and Y. Colin, *Thin Solid Films*, 182, 1989, 1-14.
25. S. K. J. Al-Ani, H. H. Mohammed and E. M. N. Al-Fwade, *Renewable Energy*, 25, 2002, 585-590.
26. S. Gogoi and K. Barua, *Jap. J.: Appl. Phys.*, 18(12), 1979, 2239.
27. P. K. Kalita, B. K. Sarma and H. L. Das, *Bull. Mater. Sci.*, 26(6), 2003, 613.
28. K. K. Singh, R. Sarma and H. L. Das, *Indian J. Phys.* 79(6), 2005, 631-633.
29. R. D. Gould and C. J. Bowler; *Thin Solid Films*, 164, 1988, 383.
30. John G. Simmons in *Hand Book of Thin Film Technology* (eds) L. I. Maissel and R. Glang, Mc Graw-Hill Book Company, N. Y. 1970, Chap 14.
31. R. W. Jansen and O. F. Sankey; *Phys. Rev. B*, 39(5), 1989, 3192.
32. A. B. Maity, S. Choudhury and A. K. Pal; *Phys. Stat. Sol.*,183, 1994, 185.
33. P. Mahawela, S. Jeedigunta, S. Vakkalanka, C. S. Ferekides and D. L. Morel; *Thin Solid Films*, 480-481, 2005, 466-470.
34. B. G. Streetman, *Solid State Electronic Device*, Prentice Hall of India (P) Ltd. New Delhi, 1995.
35. A. Grabowski, M. Nowak and P. Tzanetakis, *Thin Solid Films*, 283, 1996, 77.
36. R. H. Bube, *Photoconductivity in Solids*, Wiley, N. Y. 1960, P-391.

37. N. Goyal; *Ind. Jour. Pure and Appl. Phys.*, 31, 1993, 588-590.

38. A. Rose, *Concepts in Photoconductivity and Allied Problems*, Wiley Interscience, N. Y., 1963, p 38-43.

39. D. P. Padiyan, A. Marikiani and K. R. Murali, *Mat. Chem & Phys.*, 78, 2002, 51-58.

40. A. Goswami, *Thin Film Fundamentals*, New Age International Publications, New Delhi, 1996, p 279.

41. M. Burogohain and K. Barua, *Indian J. of Phys.*, 6/A, 1987, 559.

42. K. C. Sarma, R. Sarma and J. C. Garg, *Jap. J. App. Phys.*, 31,1992, 742.

43. K. C. Sathyalatha, S. Uthanna and P. Jayarama Reddy, *Thin Solid Films*, 174, 1989, 233-238.

44. K. N. Shreekanthan, B.V. Rajendra, V. B. Kasturi and G. K. Shivakumar; *Cryst. Res. Technol.* 38(1), 2003, 30-33.

45. S. A. Mahmoud, A. Ashour and E. A. Badawi, *Appl. Sur. Sci.*, 253, 2006, 2969-2972.

46. R. H. Bube, *Photoconductivity in Solids*, Wiley, N.Y. 1960, Chap. 9.

47. L. B. Freund and S. Suresh; *Thin Film Materials - Stress, Defect Formation and Surface Evolution*, Cambridge University Press, 2003.

****